

Palynology of core 1-AS-20-AM from the Miocene and Quaternary of western Amazonia

CARLOS D'APOLITO^{1,2*}, SILANE A.F. da SILVA-CAMINHA¹
and CARLOS JARAMILLO³

¹Faculty of Geosciences (FAGEO), Universidade Federal de Mato Grosso (UFMT), Cuiabá, MT, Brazil; e-mails: carlosdapolito@gmail.com, ORCID: 0000-0003-1602-0201; silane.silva@gmail.com, ORCID: 0000-0003-4853-2789

²Center for Natural and Biological Sciences (CCBN), Universidade Federal do Acre (UFAC), Rio Branco, AC, Brazil

³Center for Tropical Paleontology and Archeology (CTPA), Smithsonian Tropical Research Institute (STRI), Ancon, Panama City, Panama; e-mail: JaramilloC@si.edu, ORCID: 0000-0002-2616-5079

Received 17 May 2024; accepted for publication 10 September 2024

ABSTRACT. The western Amazon landscapes evolved during the Neogene–Quaternary in response to the effects of the Andean orogeny and dynamic topography. During the Miocene, sedimentary basins accumulated hundreds of meters of sediments that harbor the biological history of the region and, consequently, the emergence of the amazonian biome. Palynology is the main source of biostratigraphic and paleobotanical information, its use has allowed placing sedimentary and biological events during the Miocene in a chronological framework. Here, we present palynological data from core 1-AS-20-AM, located in the northeastern portion of the Solimões Basin and exposing the Solimões and Içá formations of Miocene and Pleistocene ages, respectively. Pollen samples were collected throughout the 286 meters of core and processed following standard palynology methods. We report well-known index species from zonation schemes in Colombia and Venezuela, adapted for use in western Amazonia, and place the Solimões Formation in core 1-AS-20-AM into the Middle to Late Miocene. The occurrence of *Cyatheacidites annulatus*, marker of zone T17, confirms the presence of the latest Miocene in the basin, recorded for the first time in cores. The Içá Formation in core 20AM is only tentatively assigned to zone T18 of Pliocene/Pleistocene age. We discuss the possibility of a six-million-year hiatus between the formations. Several species are recorded at a topmost extant (Holocene) sample and can serve as calibration for last appearance events. We also detected a Middle Miocene marine incursion along ~60 meters at the bottom of the core. Ten new taxa are erected formally, some of which had been recorded informally elsewhere and will be useful for future biostratigraphic correlations. The new species also document the first occurrences of two plant groups for the Miocene of Amazonia, they are related to *Cabomba* (Cabombaceae), and *Eichhornia/Pontederia* (Pontederiaceae). The new data from core 1-AS-20-AM will be key for regional biozonation schemes and analyses of biodiversity emergence.

KEYWORDS: pollen, spores, Amazon, Solimões Formation, Içá Formation

INTRODUCTION

Sedimentary basins in western Amazonia are well known for their rich Neogene fossil record (Antoine et al., 2016; Hoorn et al., 2023). In this region, palynology has played a key role in biostratigraphy, landscape and climatic reconstructions, as well as plant evolution (Hoorn, 1993; Jaramillo et al., 2017;

Silva-Caminha et al., 2020; Espinosa et al., 2020; Gomes et al., 2022; D'Apolito et al., 2022). First age determinations using pollen and spores were attempted by Maia et al. (1977) for the Solimões Formation in western Brazilian Amazonia (Cruz, 1984), and were based on an Atlantic coast palynological zonation (Regali et al., 1974). They concluded a Miocene to Pliocene age, which was later refined

* Corresponding author

by Hoorn (1993), who adapted a zonation from Venezuela (Lorente, 1986) for use in western Amazonia (e.g. Silva-Caminha et al., 2010; Leite et al., 2017; Leandro et al., 2019, 2022). More recently, cores from the Solimões Formation have been correlated with a palynological zonation from the Llanos Basin in Colombia (Jaramillo et al., 2011), with further refinement of ages (Jaramillo et al., 2017; Leite et al., 2021; Espinosa et al., 2021).

From the landscape evolution viewpoint, much debate has developed around the existence of marine incursions (e.g. Hoorn, 1993; Latrubesse et al., 2010; Jaramillo et al., 2017 and references therein). Palynology, again, has been essential to resolve the question, showing that short-lived spikes of dinocysts and foraminiferal linings in western Amazonia could be correlated with the same events in the Colombian Llanos during Early and Middle Miocene (Boonstra et al., 2015; Jaramillo et al., 2017). There is also some evidence for a Late Miocene incursion (Espinosa et al., 2021; Leandro et al., 2022) that is still controversial.

The vegetation that dominates the region, as reconstructed by pollen data, indicates a wetland system, called the Pebas System. Most of the pollen in sediments of the Solimões Formation seems to be sourced from the local flooded vegetation, with a smaller but detectable portion from uplands, including the high Andes (Hoorn, 1993; D'Apolito et al., 2021; Gomes et al., 2021; Hoorn et al., 2022b). Changes from swamp-dominated wetlands to fluviolacustrine systems are also evident from palynological data (Leite et al., 2017; D'Apolito et al., 2021; Hoorn et al., 2023), and floristic comparisons suggest a homogeneous vegetation at continental scale compared to at present (Gomes et al., 2021), although cycles of vegetation change have been recorded at local scales (Hoorn et al., 2022b). Pollen-based climatic reconstructions indicate warm and humid conditions throughout the late Early to early Late Miocene (Gomes et al., 2022).

There is still too much to learn about the biome that once occupied western Amazonia during most of the Miocene (the Pebas System). Sampling efforts still need to be increased (D'Apolito et al., 2021; Gomes et al., 2021) and known botanical affinities of the fossil taxa are still quite low, around 40% or less (D'Apolito et al., 2021; Espinosa et al., 2021). The aim of

this contribution is to present the palynology of core 1-AS-20-AM, from the Solimões Formation, which will be a key site for any local zonation scheme.

GEOLOGICAL SETTING

The Solimões Formation is located in the Solimões Basin in western Brazilian Amazonia (Fig. 1A). The basin is intracratonic and has accumulated sediments since the Ordovician (Wanderley-Filho et al., 2007), while the last phase of sedimentation started in the Cretaceous and has been affected by the orogeny of the Andes, especially in the latest Oligocene to Pliocene times (Hoorn et al., 2010). Many neighboring basins have laterally equivalent deposits of Miocene age as well (Fig. 1A). The Solimões Formation crops out in numerous locations along the main rivers of western Amazonia, including the homonymous Solimões River in Brazil; in Peru it is known as Pebas Formations and in Colombia as “Terciário Amazonico” (Hoorn, 1993). In general, there is a southwestern thickening trend (Fig. 1B) – in the Acre Basin, maximum depths can attain >2000 m (Feijó and Souza, 1994; Silva-Caminha et al., 2020), however, in most of the basin the Solimões reaches no more than 500 m (Maia et al., 1977; Fig. 1B). Sediments vary from greenish and grayish mudstones and siltstones, interbedded with gray to yellowish sands, and less often limestone and lignite. They accumulated in lacustrine to fluvial settings with short shallow marine episodes (see Introduction). A wealth of fossils has been retrieved from the Solimões beds, from large-sized caimans (Paiva et al., 2022) and mammals (Negri et al., 2010) to endemic mollusks and ostracods (Wesselingh et al., 2006; Wesselingh and Ramos, 2010). Palynology and South American Land Mammal Ages (SALMA) point to ages from the Early to Late Miocene (Cruz, 1984; Hoorn, 1993; Jaramillo et al., 2010; Latrubesse et al., 2010). Absolute ages are only available from detrital zircon populations in two outcrops in the Acre Basin (Bissaro-Jr., et al. 2019) and core 1-AS-14-AM at ~95 m depth (Kern et al., 2020; Fig. 1B), both pointing to maximum ages in the Late Miocene for deposition of the upper Solimões Formation.

The Solimões Formation can sometimes be topped by Quaternary deposits, some of which are recognized as the Içá Formation (Maia

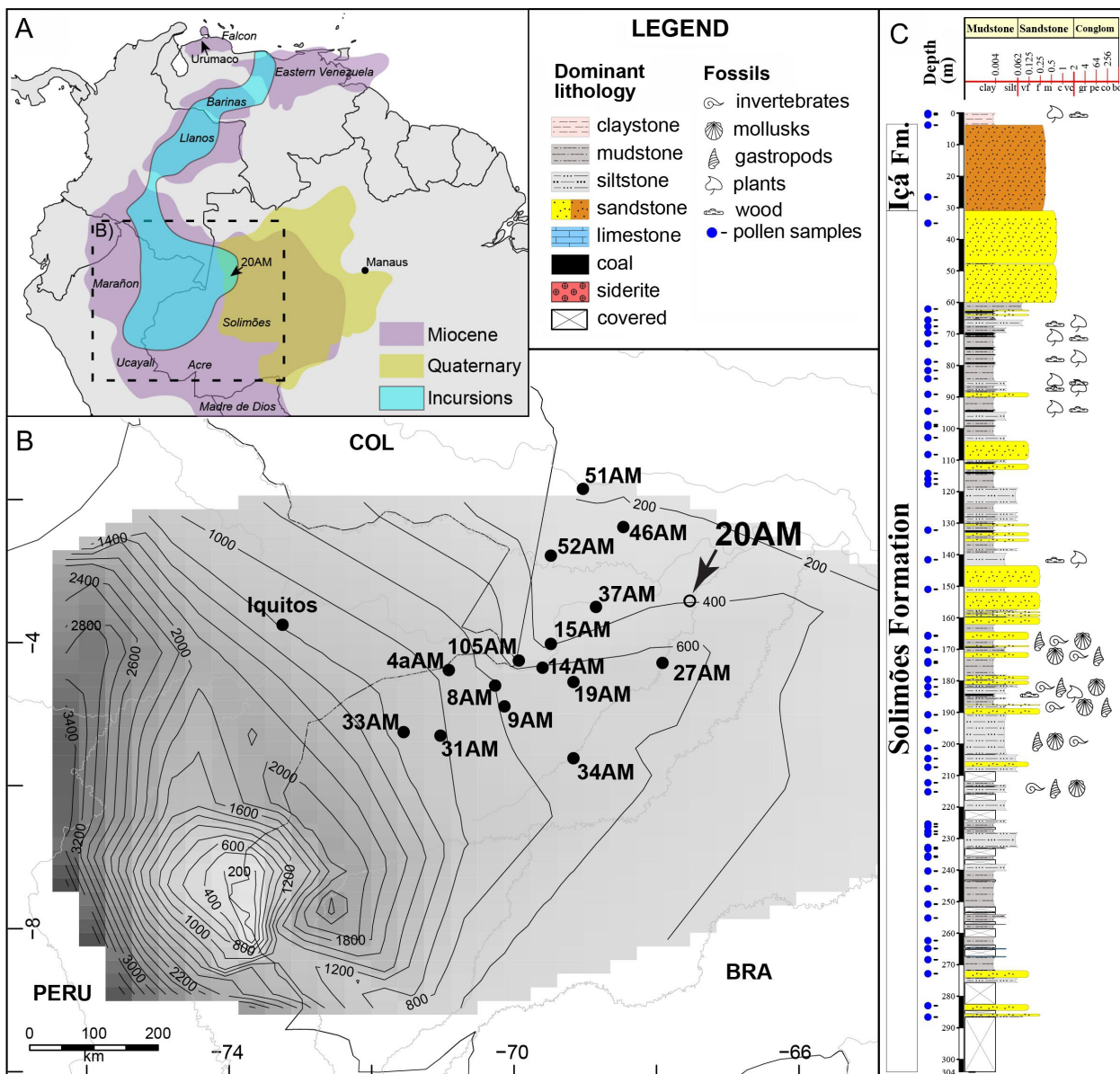


Figure 1. Location map. **A.** northwestern South America highlighting the Solimões (Miocene) and Içá (Quaternary) formations. Basin names in italic. Marine incursion extent adapted from Jaramillo et al. (2017) with adaptations from Silva-Caminha et al. (2020) and the present study; **B.** isopach map of the Miocene deposits in western Amazonia, adapted from Silva-Caminha et al. (2020), and location of cores where palynology was studied: 4aAM (Hoorn, 1993), 8AM (Linhares et al., 2019), 9AM (Espinosa et al., 2021), 14AM (Kern et al., 2020), 15AM (Gomes et al., 2021), 19AM (Silva-Caminha et al., 2010), 27AM (Silva-Caminha et al., 2010), 31AM (Kachniasz and Silva-Caminha, 2016), 33AM (Leite et al., 2021), 34AM (Kachniasz and Silva-Caminha, 2016), 37AM (Leite et al., 2021), 46AM (Sá et al., 2020), 51AM (Leandro et al., 2022), 52AM (Leandro et al., 2022), 105AM (D'Apolito et al., 2021); **C.** log of core 20AM and position of pollen samples, log performed using SDAR (Ortiz and Jaramillo, 2020) for R

et al., 1977). The Içá is characterized as highly oxidized sandstones and is non-fossiliferous. It extends over 1,000,000 km² from western to central Brazilian Amazonia (Reis et al., 2006) and commonly lies unconformably on the Solimões Formation. Age has been inferred as Pliocene-Pleistocene due to the stratigraphic relationship with the basal Miocene and overlying Late Pleistocene to Holocene beds, however, optically stimulated luminescence (OSL) dates have restricted it to the Mid-Late Pleistocene (Rossetti et al., 2015; Pupim et al., 2019).

A series of boreholes were drilled by the Brazilian Geological Survey (CPRM) in the 1970s (Maia et al., 1977) and many have already been studied for palynology (Fig. 1B). Here, we present core 1-AS-20-AM (hereafter 20AM), which was drilled along the Jutaí River (-67.533° , -3.416°) at an altitude of 73 m a.s.l. Its original description was performed by Maia et al. (1977). The core recovered both Solimões and Içá deposits, having reached 304 m, with about 62.5% of recovery rate. The Solimões Formation spans from 304 to 31 m, and is

characterized by muds, silts, sands and less often limestones and lignites (Fig. 1C). The Içá Formation spans from 31 to 3.5 m and is composed of a massive fine to medium-grained reddish sandstone package. The first 3.5 m of core are recent clays of likely Holocene age (Maia et al., 1977).

MATERIAL AND METHODS

We sampled core 20AM in 2012 at the facilities of CPRM in Manaus. Layers chosen were those of finer and more organic (darker) sediments, sandstones were also collected when they displayed a finer and dark matrix. From a total of 201 samples, we selected 58 for pollen analyses and 56 of them were productive. The Solimões Formation included 54 samples and the Içá and Holocene beds were represented by one productive sample each. Laboratory procedures followed standard techniques with acid dissolution, panning and sieving (Riding, 2021), without the use of centrifuge, and were conducted by Paleoflora® in Colombia. We aimed at counting at least 300 palynomorphs per sample when possible, and identified them using regional literature (e.g. D'Apolito et al., 2021) and the Smithsonian Institute online palynological database (Jaramillo and Rueda, 2023). We compared biostratigraphic events of First Appearance Datum (FAD) and Last Appearance Datum (LAD) in core 20AM with the same events in the Llanos Basin zonation (Jaramillo et al., 2011) and in core 105AM (Fig. 1B; Jaramillo et al., 2017). Due to a debate of ages of marine incursions (Espinosa et al., 2021; Leandro et al., 2022), we did not use marine palynomorph spikes as age markers.

Some new pollen and spore were described when they were of unique morphology, easy to recognize, had been reported as informal in core 105AM (Jaramillo et al., 2017), or had a known botanical affinity. Terminology followed Punt et al. (2007) and Jaramillo and Dilcher (2001). All specimens come from core 1-AS-20-AM, unless otherwise noted. We use the England Finder (EF) coordinate system, slides are stored at the repository of the Paleontology and Palynology Laboratories of the Universidade Federal de Mato Grosso (UFMT) in Cuiabá, MT, Brazil. Photomicrographs were performed with a Canon EOS Rebel t5 on a Zeiss Axioplan2 microscope at a magnification of 100×; illustrated specimens are new species, biostratigraphic markers, species that had been recorded only once or illustrated poorly in the literature.

RESULTS

The Solimões Formation included 54 samples with very good preservation and counts averaging ~300 palynomorphs. The samples from the Içá bed and from the Holocene yielded 67 and 252 palynomorphs, respectively.

Altogether, a total of 16,625 palynomorphs and 283 taxa were counted (Raw data counts can be accessed at <https://doi.org/10.6084/m9.figshare.26273662> (D'Apolito, 2024)). They include two algae, *Botryococcus* and *Pediasium*; 14 dinoflagellate cysts and acritarchs; 206 angiosperm and one gymnosperm pollen; and 60 fern spores. We also found six reworked taxa of three age groups: Paleozoic (*Ammonidium* sp.), Cretaceous (*Callialasporites dampieri*, *Elaterosporites klaszi*, *Gnetaceaepollenites diversus*, and *Oligosphaeridium* sp.) and Paleogene (*Cicatricosisporites dorogensis*).

Biostratigraphic marker species of zone T14, *Grimsdalea magnaclavata* (Fig. 2) was found from the basal sample at 286.6 m, and *Crassoretitriletes vanraadshooveni* (Fig. 2), which marks zone T15, was found from depth 272.85 m. At the same depth, the FAD of *Psilastephanoporites tesseroporus* (Fig. 2) was found, which is also present at the base of zone T15 (Jaramillo et al., 2011). The marker of zone T16, *Fenestrites spinosus* (Fig. 2), has a FAD at 114.2 m, and the marker species of zone T17, *Cyatheacidites annulatus* (Fig. 2), at 34.9 m. These zones indicate that core 20AM ranges from Middle to Late Miocene. The marine event at the base of the core, from 286.6 to 225.4 m, is related to the Middle Miocene flooding (Jaramillo et al., 2017). In this interval, 15 out of 18 samples have marine indicators with an average of 48% (Figs 2 and 3). The sum of marine palynomorphs included Leiospheres after noticing that they correlated well with the total sum of dinocysts ($r^2 = 0.65$, $p < 0.01$).

Limited inferences about the age of the Içá Formation can be drawn from core 20AM, which is due to a single sample with low count ($n = 67$). The presence of *Paleosantalaceapites cingulatus* could be interpreted as its LAD event and correlated with basal zone T18 (Jaramillo et al., 2011). The topmost sample (Holocene) is useful to record taxa from the Solimões and Içá formations that still exist today in the region, including *Cingulatisporites cristatus*, *Camarozonosporites fossulatus*, *Tetracolporopollenites silvaticus*, *Ranunculacidites operculatus*, *Psilamonocolpites nanus*, *Psiladiporites redundantis*, *Proteacidites poriscabratus*, *Multiporopollenites crassinexinatus*, *Echitricolporites spinosus*, *Crotonoidaepollenites reticulatus*, *Cichoreacidites longispinosus* and *Arecipites regio*.

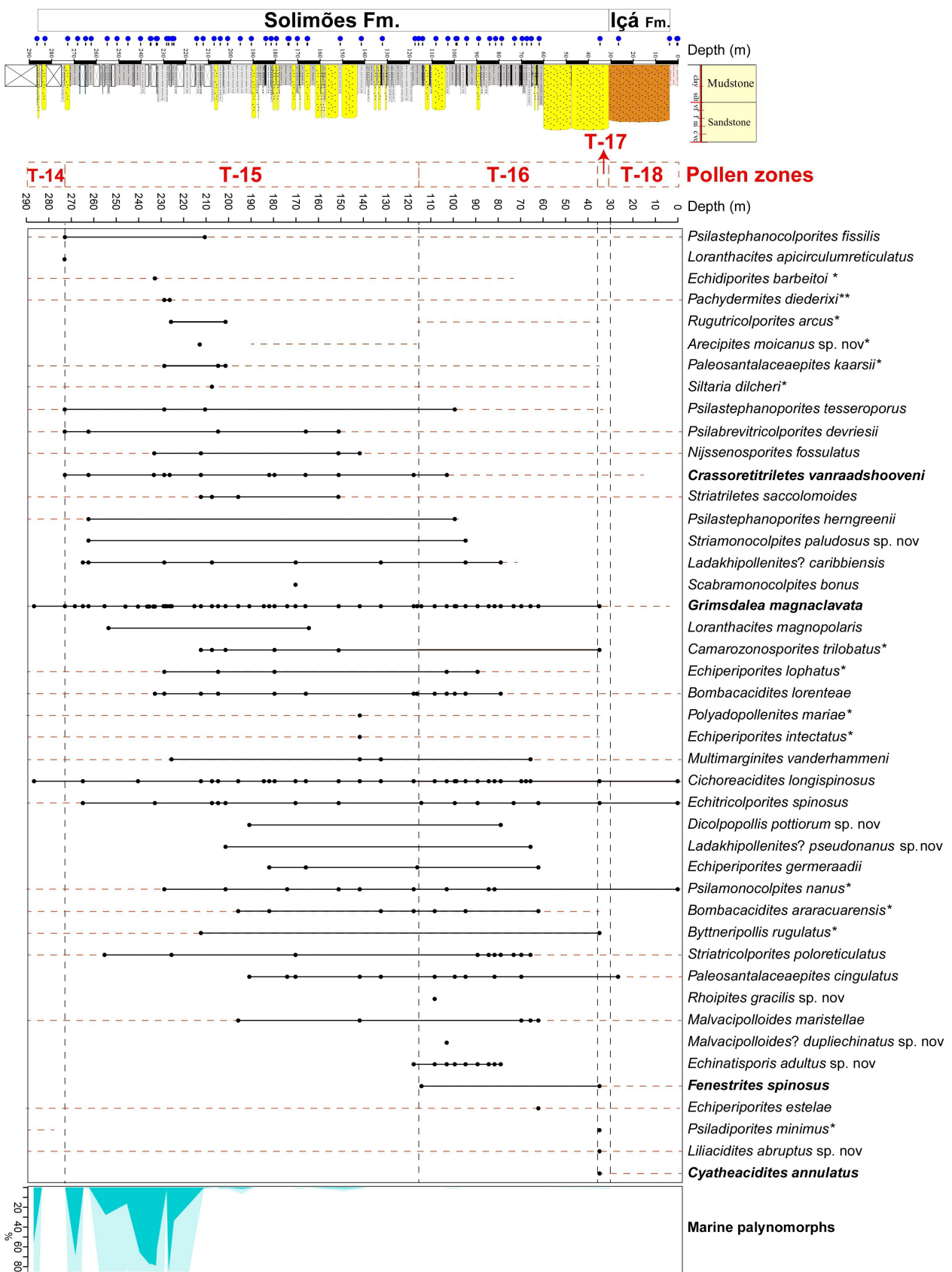


Figure 2. Range chart of selected taxa from core 20AM, Solimões Basin, Brazil. Pollen zones follow Jaramillo et al. (2011). Dashed-red lines are range of taxa according to Jaramillo et al. (2011) or compared to core 105AM (Jaramillo et al., 2017) when taxon is marked with asterisk. Relative abundance of marine palynomorphs based on total palynomorph count

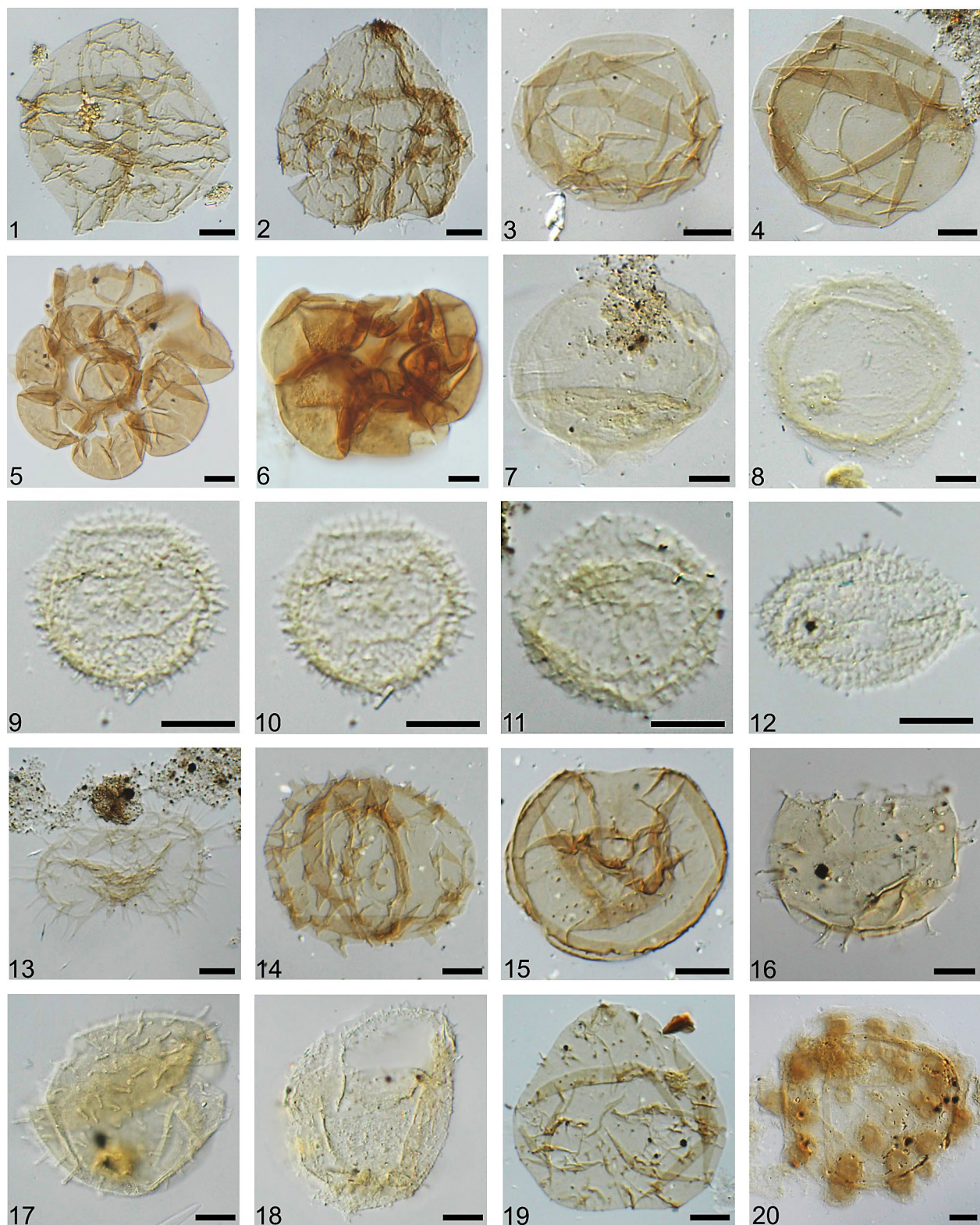


Figure 3. Photomicrographs of dinoflagellate cysts, foraminiferal linings and leiosphaeres from core 1-AS-20-AM, Solimões Basin, western Brazilian Amazonia. **1, 2.** *Cristadinium* sp., 1. sample 23920, EF K13-3; 2. sample 23964, EFK34; **3, 4.** Dinocyst brown (RBCs), 3. sample 23904, EFH5, 4. sample 23904, EF T46; **5, 6.** Foraminiferal linings, 5. sample 23907, EF R50-3/4, 6. sample 23952, EF F45-4; **7, 8.** *Leiosphaeridia* spp., 7. sample 23904, EF O43-4, 8. sample 23904, EF Q6-3/4; **9–12.** *Nanobarbophora* sp., 9, 10. sample 23904, EF S37-1, 11. sample 23912, EF Q41-2, 12. sample 23904, EF Q38-3; **13.** *Quadrina?* *condita* de Verteuil et Norris 1996, sample 23904, EF G8-4; **14.** *Quadrina?* *triangulata* Cárdenas et al. 2021, sample 23934, EF L8; **15.** *Selenopemphix* sp., sample 23920, EF J21-1/2; **16.** *Spiniferites* sp., sample 23901, EF N36; **17.** *Lingulodinium machaerophorum* (Deflandre et Cookson 1955) Wall 1967, sample 23912, EF Q40-1/2; **18.** *Operculodinium* spp., sample 23901, EF V26-3/4; **19.** *Trinovantedinium ferugnomatum* de Verteuil et Norris 1996, sample 23920, EF M19-1/3; **20.** *Tuberculodinium vancampoae* (Rossignol 1962) Wall 1967, sample 23952, EF K17-2/4. All scale bars = 10 µm

SYSTEMATIC PALYNOLOGY

SPORES

Genus *Echinatisporis* Krutzsch 1959

Type species *Echinatisporis longechinus* Krutzsch 1959

***Echinatisporis adultus* sp. nov.**

Fig. 4.9–4.12

Holotype. Sample 23776, EF Y8-1/2, Fig. 4.9 and 4.10.

Paratype. Sample 23788, EF V49-1/3, Fig. 4.11 and 4.12.

Diagnosis. Polar shape circular to triangular-obtuse-convex; trilete; symmetry radial; laesurae slightly undulating, commissure indistinct; echinate; ornamentation 2.6 µm (2–3, n = 7); echinate to baculate, echinae thin, 2 µm tall, <1 µm wide, ~2 µm apart, distributed densely and evenly over all surface; 1-layered; exospore thickness 1.1 µm (1–1.5, n = 7).

Dimensions. Distal view length 37.1 µm (33–42, n = 7); distal view width 32.7 µm (26–38, n = 7); radii length 10 µm; Tli 0.27.

Intraspecific variability. Trilete mark often not observed. Spines more common, sometimes baculae also observed.

Comparisons. *Echinatisporis brevispinosus* Jaramillo and Dilcher 2001 has dense and larger/wider echinae; *Apiculatasporites obscurus* Jaramillo and Dilcher 2001 has echinae with large base and psilate contact area; *Planaeasporites* sp. 2 (Jaramillo and Dilcher, 2001) has uneven spines, raised laesure and scabrate intexine; *Echinatisporis muelleri* (Regali et al. 1974) Silva-Caminha et al. 2010 and *E. longechinus* Krutzsch 1959, and *E. varispinosus* (Pocock) Srivastava 1977 have much larger spines relative to spores size; *Echinatisporis minutus* van der Kaars 1983 is smaller and has larger spines relative to spore size; *E. circularis* Silva-Caminha et al. 2010 is smaller, has larger spines relative to spore size and curvatura perfecta; *E. parviechinatus* D'Apolito et al. 2019 has thicker sporoderm, longer and straight laesure; *Echitriletes minispinosus* Jaramillo et al. 2014 Informal is much smaller and has

longer radii; *E. minutuechinulatus* Jaramillo et al. 2014 Informal has smaller and denser echinae; *Echinatisporis distaequinatus* Gomes et al. 2021 has echinae restricted to distal face; *E. infantulus* D'Apolito et al. 2021 has smaller and sparse echinae, and straight laesura.

Etymology. After similarity with *E. infantulus* D'Apolito et al. 2021.

POLLEN

Genus *Arecipites* Wodehouse 1933,
emend. Nichols et al. 1973

Type species *Arecipites punctatus* Wodehouse ex Potonié 1958

***Arecipites moicanus* sp. nov.**

Fig. 5.1–5.8

Holotype. Sample 23893, EF G21, Fig. 5.1, 5.2 and 5.3.

Paratype. Sample 22279, EF H46-1/2, core 1-AS-105-AM, Fig. 5.4 and 5.5.

Specimens. Sample 22290, EF T37-3, core 1-AS-105-AM, Fig. 5.6 and 5.7; Sample 23893, EF G17-2, Fig. 5.8.

Diagnosis. Monad; polar shape ellipsoidal; isopolar; symmetry bilateral; monosulcate (monocolpate); colpus long, 34 µm, longicolpate, slightly costate, costa created by thinning of nexine, colpus can be open at one or both ends, rounded; tectate; exine 2 µm thick, nexine 0.5, columella 0.5, columellae evenly spaced, thin, tectum thick, 1 µm; psilate to perforated; heterobrochate; psilate on most of the surface except the opposite side of the aperture where an area of the mesocolpium becomes progressively foveolate to fossulate, foveola 0.5 µm, rounded, fossulae 1–2.5 µm long, 0.5 µm wide. This ornamented area protrudes due to taller columellae, area ~20 × 15 µm.

Dimensions. Polar view length 33.8 µm (32–38 µm, n = 4); polar view width 27.8 µm (26–30 µm, n = 4); colpus length 30.5 µm (25–34 µm, n = 4).

Comparisons. No monosulcate foveolate/fossulate species has a protruding exine region.

Etymology. After protruding exine like a mohican hair.

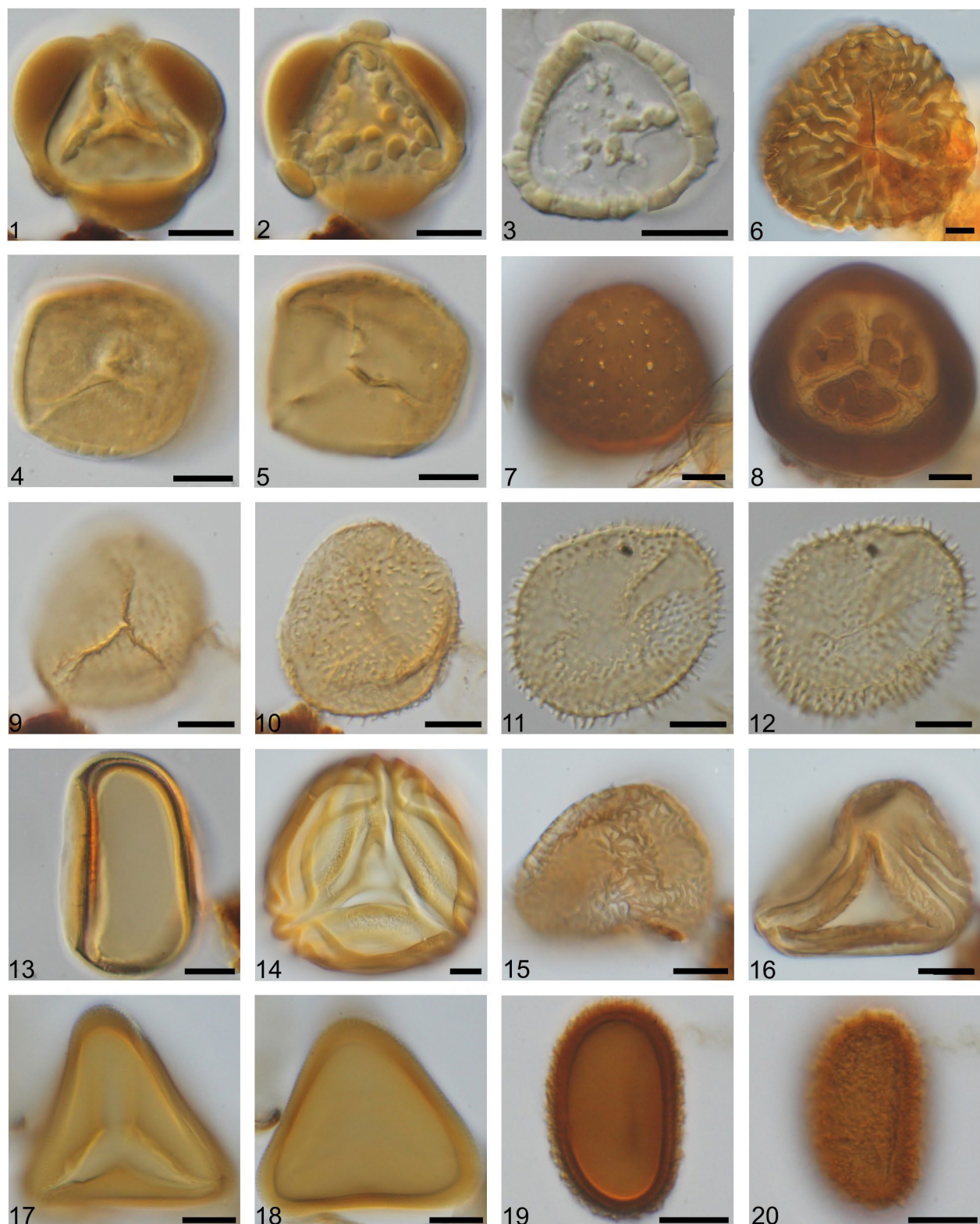


Figure 4. Photomicrographs of spores from core 1-AS-20-AM, Solimões Basin, western Brazilian Amazonia. **1, 2.** *Camerazonosporites trilobatus* D'Apolito et al. 2021, sample 23892, EF D16-3; **3.** *Cingulatisporites cristatus* D'Apolito et al. 2021, sample 23964, EF O34-2; **4, 5.** *Cingulatisporites matisiensis* D'Apolito et al. 2021, sample 23892, EF V5; **6.** *Crassoretitriletes vanraadshooveni* Germeraad et al. 1968, sample 23900, EF F34-2/4; **7, 8.** *Cyatheacidites annulatus* Cookson 1947, sample 23728, EF N47; **9, 10.** *Echinatisporis adultus* sp. nov., holotype, sample 23776, EF Y8-1/2; **11, 12.** *Echinatisporis adultus* sp. nov., paratype, sample 23788, EF V49-1/3; **13.** *Laevigatosporites cultellus* D'Apolito et al. 2021, sample 23893, EF Q5-3/4; **14.** *Magnastriatites grandiosus* (Kedves et Solé de Porta 1963) Dueñas 1980, sample 23804, EF O17; **15, 16.** *Nijssenospores fos-sulatus* Lorente 1986, sample 23826, EF U9-4; **17, 18.** *Psilatriletes marginatus* D'Apolito et al. 2021, sample 23728, EF T9-2; **19, 20.** *Punctatosporites latrubessei* D'Apolito et al. 2021, sample 23766, EF O21-3/4. All scale bars = 10 µm

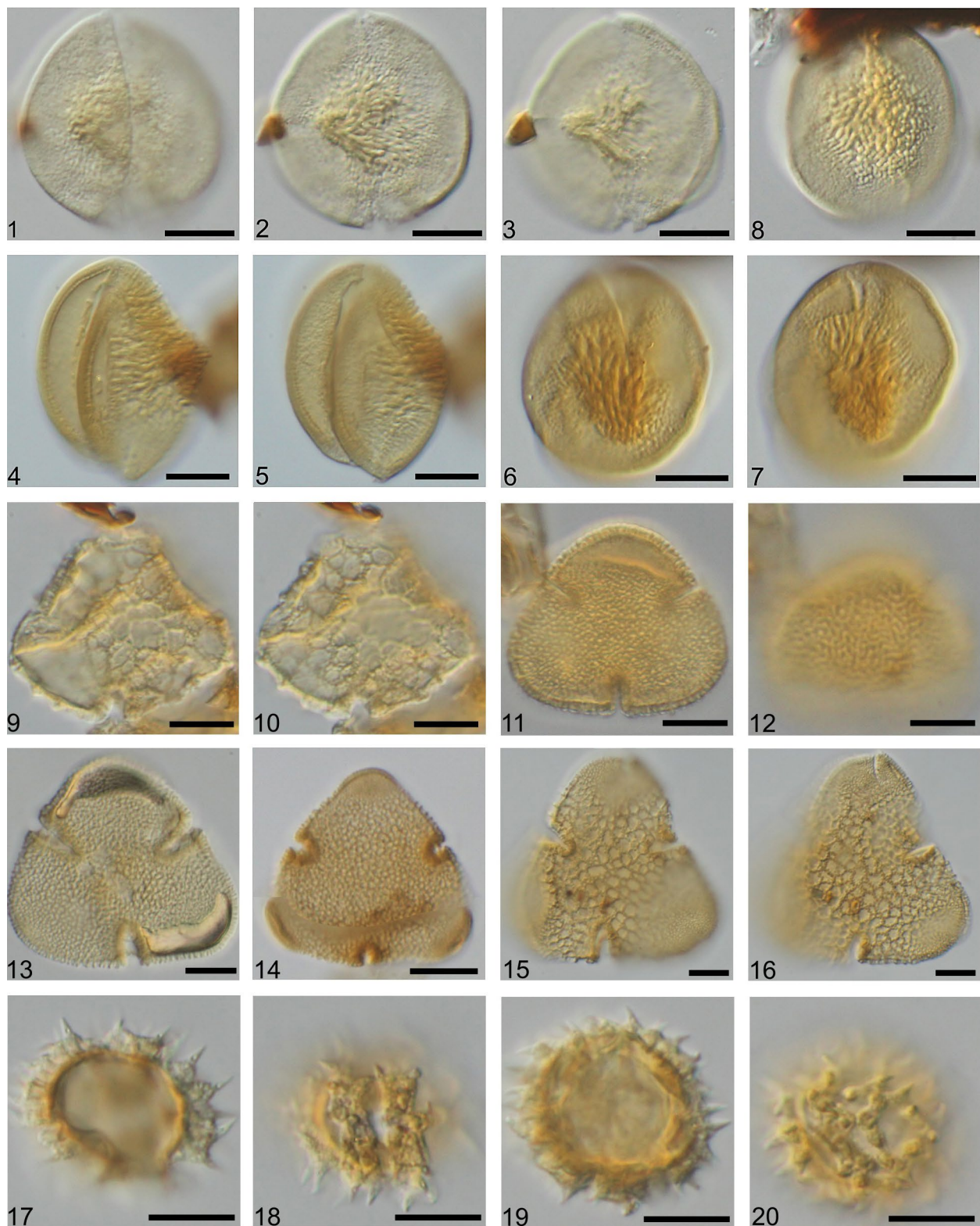


Figure 5. Photomicrographs of pollen from core 1-AS-20-AM, Solimões Basin, western Brazilian Amazonia. **1–3.** *Arecipites moicanus* sp. nov., holotype, sample 23893, EF G21; **4, 5.** *A. moicanus* sp. nov., paratype, sample 22279, EF H46-1/2, core 1-AS-105-AM; **6, 7.** *A. moicanus* sp. nov., specimen, sample 22290, EF T37-3, core 1-AS-105-AM; **8.** *A. moicanus* sp. nov., specimen, sample 23893, EF G17-2; **9, 10.** *Bombacacidites araracuarensis* Hoorn 1994, sample 23824, EF K34; **11, 12.** *Bombacacidites fossulatus* Silva-Caminha et al. 2010, sample 23824, EF M9-4; **13.** *Bombacacidites lorentae* (Hoorn) D'Apolito et al. 2021, sample 23893, EF T8-4; **14.** *Bombacacidites muinaneorum* Hoorn 1993, sample 23776, EF U8-1/3; **15, 16.** *Bombacacidites nacimientoensis* (Anderson 1960) Elsik 1968, sample 23941, EF T43-2; **17–20.** *Cichoreacidites longispinosus* (Lorente) Silva-Caminha et al. 2010, **17, 18.** sample 23824, EF V43-1/2, **19, 20.** sample 23893, EF W18. All scale bars = 10 µm

Genus *Dicolpopollis*
Pflanzl 1956 emend. Potonié 1966

Type species *Dicolpopollis kockeli*
Pflanzl 1965

***Dicolpopollis pottiorum* sp. nov.**

Fig. 6.1–6.8

Holotype. Sample 23871, EF H18, Fig. 6.1–6.3.

Paratype. Sample 23766, EF F34-1/2, Fig. 6.4–6.6.

Specimen. Sample 23766, EF T23-1, Fig. 6.7 and 6.8.

Diagnosis. Monad; polar shape long- ellipsoidal; anisopolar; symmetry bilateral; dicolporate; colpi long, 24–33 µm long, wider at mid-length and tapering at ends, ends pointed, not reaching poles, marginate; tectate; columellae very short, indistinct, exine 1.5–1.8 µm thick; psilate to slightly micropitted, very shallow pits scattered irregularly, almost not visible.

Dimensions. Polar view length 32 µm (28–39 µm, n = 4); polar view width 15.8 µm (13–20 µm, n = 4); colpi length 27.2 µm (24–33 µm, n = 4); colpi width 3.4 µm (1–8 µm, n = 4).

Comparisons. *Dicolpopollis?* *obtusipolus* Silva-Caminha et al. 2010 is reticulate and has distinct columellae; *Dicolpopollis malesianus* Muller 1968 and *D. elegans* Muller 1968 are longicolporate and reticulate; *Psiladicolpites comptus* Regali 1989 has distinct stratification and exine thickens towards mesocolpium.

Natural Affinity. *Eichhornia/Pontederia* (Pontederiaceae) (Fig. 6.9–6.12). The dicolporate and long- ellipsoidal morphology seems to match some Pontederiaceae genera, which were chosen as most likely extant affinity with the fossil. Other dicolporate extant pollen are different, for instance *Dioscorea* (Dioscoreaceae) has circular equatorial contour and the ornamentation much more developed (Alzer et al., 2001); Some Lepidocaryoid palm genera also have dicolporate grains, but ornamentation is much coarser, ranging from reticulate, verrucate to baculate, clavate (Zavada, 1983); dicolporate pollen is observed in the Araceae, but also with different shape and ornamentation

patterns (Zavada, 1983; Ulrich et al., 2013); *Pedicularis* (Orobanchaceae) has sunken colpi with an ornamented aperture membranae (Halbritter and Heigl, 2021)

Etymology. After Brazilian botanists Vali J. Pott and Arnildo Pott.

Genus *Ladakhipollenites*
Mathur et Jain 1980

Type species *Ladakhipollenites levis*
(Sah et Dutta 1966) Mathur et Jain 1980

***Ladakhipollenites?* *pseudonanus*
sp. nov.**

Fig. 7.18–7.20

Holotype. Sample 23883, EF N29-1, Fig. 7.18.

Paratype. Sample 23733, EF O16, Fig. 7.19.

Specimen. Sample 22412, EF D8-1, core 1-AS-105-AM, Fig. 7.20.

Diagnosis. Monad; prolate; isopolar; symmetry radial; tricolporate; colpi long, almost as long as polar axis, simple to costate, ends pointed; pores circular to slightly elliptical, small, ~1.9 µm across, simple; exine tectate, 1 µm, nexine, columellae and tectum 0.3 µm each; psilate.

Dimensions. equatorial view length 15.8 µm (12–19 µm, n = 5); equatorial view width 8.8 µm (6–11 µm, n = 5). colpi length 13 µm (10–15 µm, n = 5); pore length 1.9 µm (1.5–2 µm, n = 5); pore width 1.8 µm (1.5–2 µm, n = 5).

Comparisons. *Psilatricolporites varius* Duenas 1983 is oblate and has simple colpi and circular pores only; *Ladakhipollenites nanus* D'Apolito et al. 2021 is tricolporate; *Tetracolporopollenites nanus* D'Apolito et al. 2021 is oblate, has a broad and flattened polar area and larger pores relative to grain size; *Psilatricolporites vanus* Gonzalez 1967 is spherical, has large polar area and colpi are shorter; *P. divisus* Regali et al. 1974 is larger and has slit-like pores forming endocingulum; *P. optimus* Gonzalez 1967 is larger and has perforations in the tectum; *P. pachydermatus* Lorente 1986 is larger, has shorter colpi and slit-like pores; *Tetracolporopollenites maculosus* (Regali et al. 1974) Jaramillo et Dilcher 2001 has short colpi and lalongate

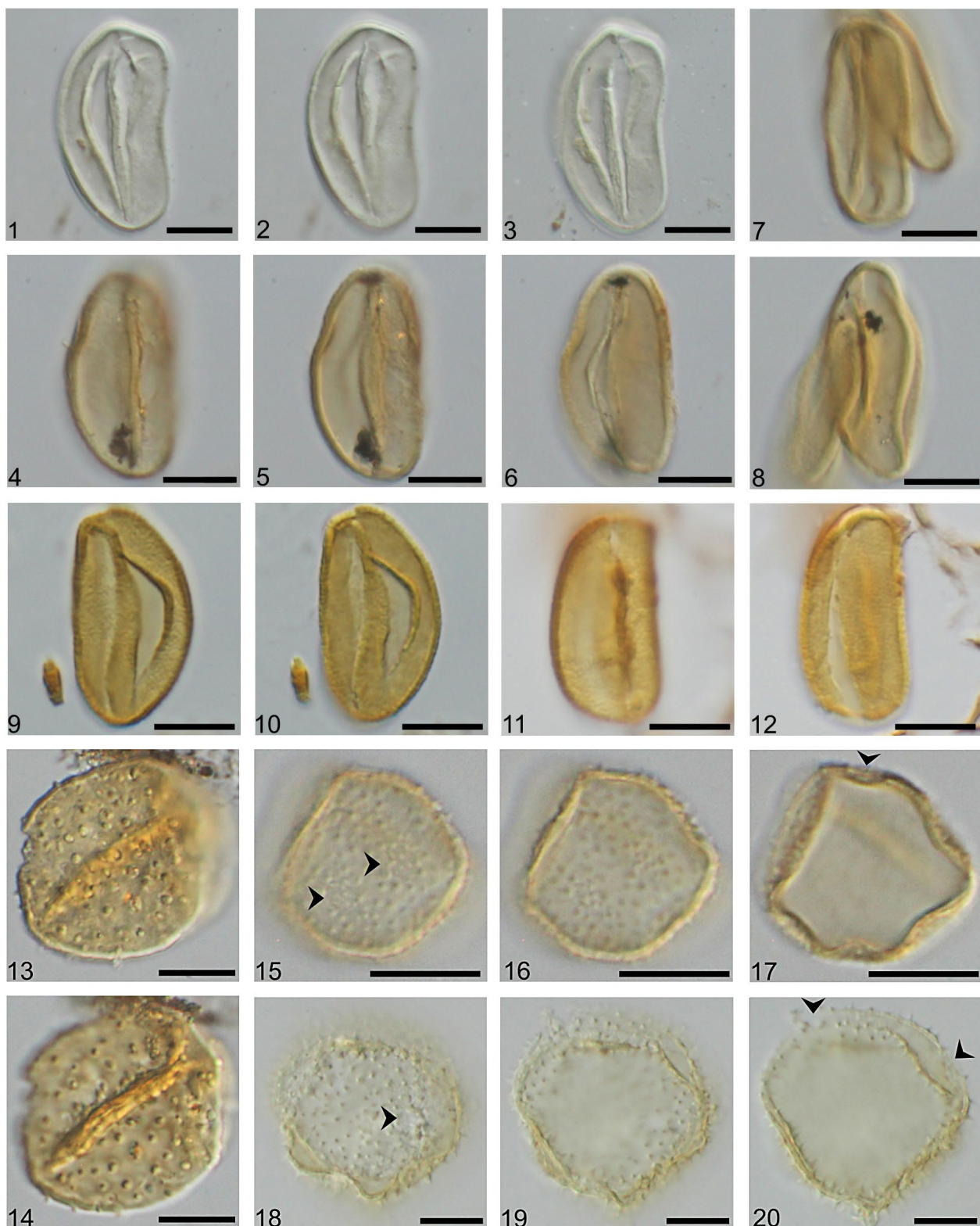


Figure 6. Photomicrographs of pollen from core 1-AS-20-AM, Solimões Basin, western Brazilian Amazonia. **1–3.** *Dicolpopollis pottiorum* sp. nov., holotype, sample 23871, EF H18; **4–6.** *D. pottiorum* sp. nov., paratype, sample 23766, EF F34-1/2; **7, 8.** *D. pottiorum* sp. nov., specimen, sample 23766, EF T23-1; **9–12.** *Eichhornia crassipes* (Mart.) Solms, Pontederiaceae (CGMS46557_PALMA1134); **13, 14.** *Echidaporites barbeitoi* (Muller et al. 1987) D'Apolito et al. 2021, sample 23904, EF P12; **15–17.** *Echiperiporites akanthos* Van der Hammen et Wymstra 1964, sample 23788, EF C15; **18–20.** *Sagittaria rhombifolia* Cham., Alismataceae (CGMS55742_PALMA997); arrows in 15, 17 18 and 20 point to pores, note the similarity of these two pantoporate grains, *Sagittaria* is a likely affinity of the fossil *E. akanthos*. All scale bars = 10 µm

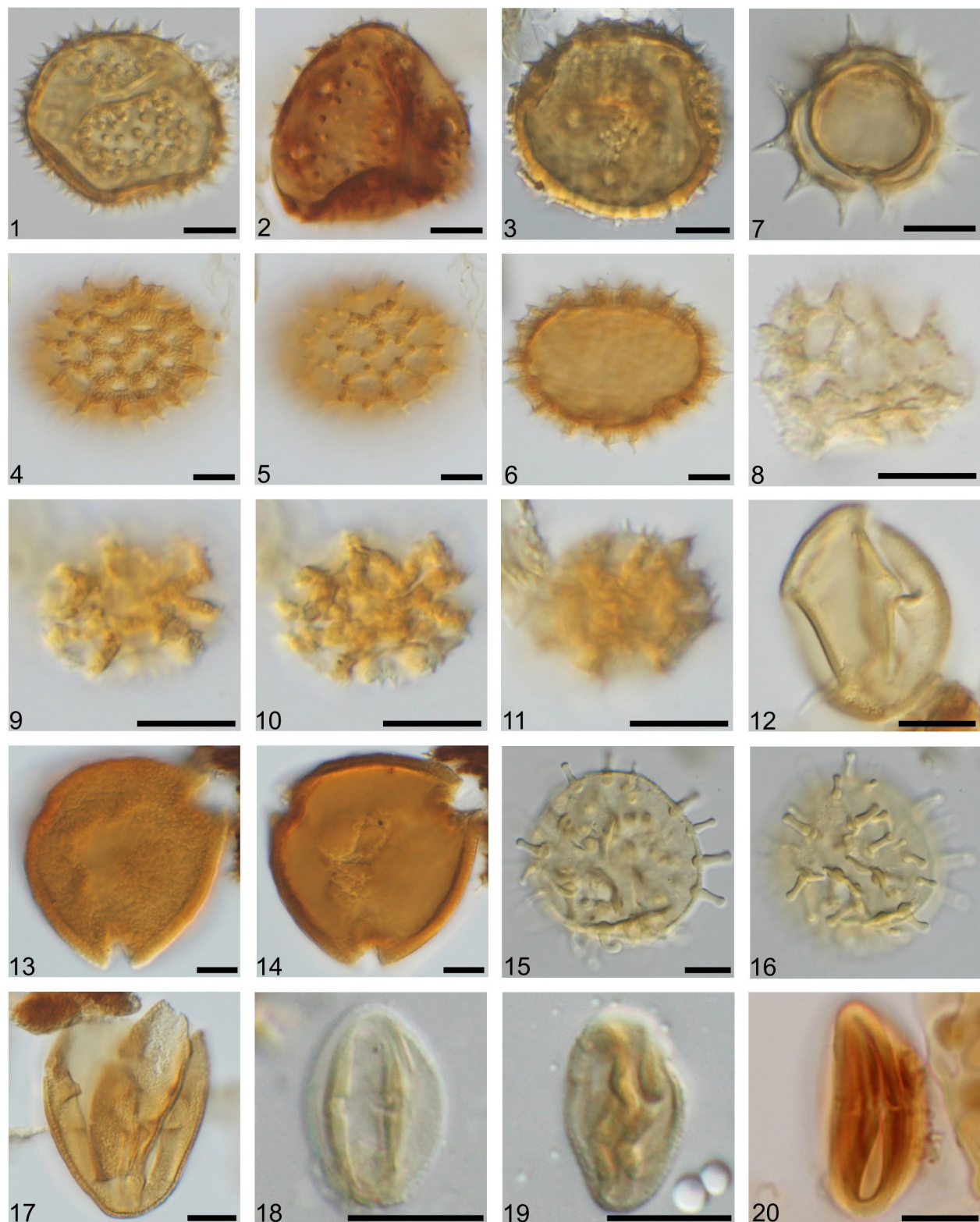


Figure 7. Photomicrographs of pollen from core 1-AS-20-AM, Solimões Basin, western Brazilian Amazonia. **1.** *Echiperiporites estelae* Germeraad et al. 1968 (sample 23729, EF Y42-4); **2.** *Echiperiporites germeraadii* Leite et al. 2021 (sample 23729, EF O9-2); **3.** *Echiperiporites jutaiensis* Silva-Caminha et al. 2010 (sample 23826, EF H6-1); **4–6.** *Echiperiporites lophatus* Silva-Caminha et al. 2010 (sample 23788, EF S43-2); **7.** *Echitricholporites spinosus* Van der Hammen 1956 (sample 23815, EF M18); **8–11.** *Fenestrites spinosus* Van der Hammen 1956 (8-sample 23728, EF K3-4; 23815, EF S19); **12.** *Foveotricolporites colpiconstrictus* (Hoorn 1994) D'Apolito et al. 2021 (sample 23956, EF W6-3/4); **13, 14.** *Foveotricolporites crassus* Leite et al. 2021 (sample 23902, EF N29-1); **15, 16.** *Grimsdalea magnaclavata* Germeraad et al. 1968 (sample 23938, EF L9); **17.** *Lada-hippocrate?* *caribbiensis* (Muller et al. 1987) Silva-Caminha et al. 2010 (sample 23840, EF L8-2/4); **18.** *Lada-hippocrate?* *pseudonanus* sp. nov. (Holotype, sample 23883, EF N29-1); **19.** *L.?* *pseudonanus* sp. nov. (Paratype: sample 23733, EF O16); **20.** *L.?* *pseudonanus* sp. nov. (Specimen: sample 22412, EF D8-1, core 1-AS-105-AM). All scale bars = 10 µm

pores; *Tetracolporopollenites* sp. 1 (Jaramillo and Dilcher, 2001) has strongly costate colpi, and large lalongate pores; *Psilatricolporites atalayensis* Hoorn 1993 has lalongate pores; *Tetracolporopollenites labiatus* (Hoorn 1993) D'Apolito et al. 2021 has broad polar areas, short colpi and protruding pores; *Tetracolporopollenites magniporatus* (Hoorn 1993) D'Apolito et al. 2021 is larger and has much larger pores relative to grain size; *Horniella megaporata* Silva-Caminha et al. 2010 has larger pores relative to grain size; *Psilatricolporites protrudus* Kar and Singh 1986 is larger and brevicolpate; *Ladakhipollenites? densicolumellatus* D'Apolito et al. 2019 has dense columellate exine, strongly costate colpi and forms endocingulum.

Etymology. After superficial similarity to *Ladakhipollenites nanus* D'Apolito et al. 2021.

Genus *Liliacidites*
Couper 1953

Type species *Liliacidites kaitangataensis*
Couper 1953

Liliacidites abruptus sp. nov.

Fig. 8.1–8.3

Holotype. Sample 23728, EF J9-1/3, Fig. 8.1–8.3.

Synonymy. *Bromeliacidites* sp. 1, Jaramillo et al., 2014.

Diagnosis. Monad; polar shape wide-elliptic; anisopolar; symmetry asymmetric; monosulcate (monocolpate); colpus long, 36 µm, tapering, with rounded ends, simple, wide, extending nearly entire length of grain, margins masked by reticulum; semitectate; exine thinner at poles, 1 µm, nexine, columellae and tectum ~0.3 µm each; exine thicker at mesocolpium, 1.5 µm, nexine, columellae and tectum 0.5 µm each. Columellae distinct, well-spaced at mesocolpium; reticulate, strongly heterobrochate, lumina becomes sharply wider from poles to mesocolpium, 1–4 µm wide, rounded to sub-polygonal, smaller lumina sometimes seen among larger ones, muri of constant width ~1 µm wide, simplicolumellate; micro-reticulate to micropitted at poles, lumina rounded, ~0.5 µm wide.

Dimensions. polar view length 46 µm (46–46 µm, n=1); polar view width 33 µm (33–33 µm, n=1); colpus length 36 µm (36–36 µm, n=1); colpus width 4 µm (4–4 µm, n=1).

Comparisons. *Bromeliacidites* sp. 2 (Jaramillo et al., 2014) Informal is intectate and baculate; *Liliacidites exilimuratus* (Legoux 1978) Eisawi and Schrank 2008 has larger lumina in the proximal side, interspersed with smaller lumina. *Liliacidites* sp. A (Muller et al. 1987) and *Liliacidites* sp. B (Muller et al. 1987) have coarser reticulum and heterobrochate pattern is less sharp; *L. variegatus* Couper 1953 is smaller, baculate-clavate with a finer reticulum; *L. kaitangataensis* Couper 1953 is much larger and clavate-baculate; *L. dividiuus* (Pierce 1961) Brenner 1963 is smaller, more circular in outline and heterobrochate reticulum not evident; *L. aegyptiacus* Penny, 1986 is smaller and finely reticulate; *L. regularis* Archangelsky 1973 has wider lumina and lacks conspicuous heterobrochate pattern of the reticulum; *L. faragraensis* Ibrahim 1997 is smaller, with more polygonal lumina; *L. baculatus* Venkatachala and Kar 1969 is much thicker; *L. vermiculatus* Archangelsky and Zamaloa 1986 has finer ornamentation, foveolate to fossulate; *L. aviemorensis* McIntyre 1968 has much larger lumina relative to grain size, including smaller lumina at the corners of larger ones; *L. bainii* Stover in Stover and Partridge 1973 is very finely reticulate; *L. lanceolatus* Stover in Stover and Partridge 1973 has thinner exine, muri decreasing gradually and indistinct columellae at poles.

Natural Affinity. *Encholirium/Tillandsia/Vriesea* (Bromeliaceae) (Fig. 8.4). The marked reticulate, strongly heterobrochate and ellipsoidal polar shape suggest an affinity with some Bromeliaceae genera. Genera *Encholirium*, *Vriesea* and *Tillandsia* share those characteristics, plus the smaller reticula surrounding the main reticulum (Halbritter, 2016; Santos et al., 2019; Souza et al., 2021). Some genera of the Liliaceae also have similar morphologies (Kosenko, 1999; Hu et al., 2021), but the family is rare in South America, therefore we suggest a more likely affinity with Bromeliaceae.

Etymology. After abrupt difference in mesh size from meso- to apocolpium.

Genus *Loranthacites* Mtchedlishvili in Samoilovitch et Mtchedlishvili 1961

Type species *Loranthacites macrosolensis* Samoilovitch et Mtchedlishvili 1961

***Loranthacites magnopolaris* sp. nov.**

Fig. 8.6–8.9

Holotype. Sample Socorro-1097m, EF H25-2, site Urumaco, Fig. 8.6 and 8.7.

Paratype. Sample Socorro-1440m, EF O49-1/3, site Urumaco, Fig. 8.8.

Specimen. Sample 23912, EF H12, Fig. 8.9.

Diagnosis. Monad, radial, isopolar, triangular-obtuse-straight, tricolporate; colpi at angles (anguloaperturate), long, ~23 µm, almost reaching poles, costate, costa 1 µm thick and 1 µm wide; tectate, exine 1.2 µm thick, nexine 0.5 µm; columellae 0.4 µm; tectum 0.4 µm, columellae distinct, closely spaced, sometimes appearing indistinct; nexine increasing to 1 µm near the colpi; the exine thickness also at the apocolpia producing a darkness area circular in shape, 7–8 µm in diameter; psilate, sometimes columellae seen through tectum.

Dimensions. Polar view length 36.3 µm (31.6–40 µm, n=6); polar view width 34.8 µm (30.8–37 µm, n=5); colpi length 23.5 µm (14–33 µm, n=6); colpi width 1.3 µm (1–1.5 µm, n=6).

Comparisons. *Loranthacites digitatus* Da Silva et al. 2010 has columellae digitate; *L. atriensis* Jaramillo et al. 2014 Informal and *L. crassitatus* Informal (Jaramillo and Rueda, 2023) have a concave shape with thicker exine in intercolpium; *Loranthacites natalie* Salard-Cheboldaeff 1978 is demicolpate and reticulate; *Loranthaceae marginalis* Jaramillo et al. 2014 Informal is parasyncolpate with thinner exine in mesocolpium; *Loranthaceae orcytanthisis* Jaramillo et al. 2014 Informal has pseudopores in the mesocolpium area; *Loranthacites tabatingensis* D'Apolito et al. 2021 is syncolpate.

Natural Affinity. Loranthaceae.

Etymology. After thicker and darker area at apocolpium.

Genus *Malvacipolloides* Anzótegui et Garalla 1986

Type species *Malvacipolloides densiechinata* Anzótegui et Garalla 1986

***Malvacipolloides?* *dupliechinatus* sp. nov.**

Fig. 8.13–8.15

Holotype. Sample 23811, EF M8-3, Fig. 8.13–8.15.

Diagnosis. Monad; tricolporate; aperture not clear, probably tricolporate, colpi short and simple; semitectate, thin, 1 µm thick, nexine 0.5 µm, columellae ~0.3 µm, tectum ~0.3 µm; echinate; homobrochate; echinate and reticulate; echinae large, 4–5 µm tall, 4 µm wide at base, end rounded, clustered in groups of two or four; reticulate, lumina 1–2 µm wide, subpolygonal, muri ~0.5 µm wide, simplicolumellate.

Dimensions. Equatorial view length 56 µm (56–56 µm, n=1); equatorial view width 60 µm (60–60 µm, n=1); colpi length 26 µm (26–26 µm, n=1); colpi width 5 µm (5–5 µm, n=1); pore length 10 µm (10–10 µm, n=1); pore width 5 µm (5–5 µm, n=1).

Comments. The species is placed provisionally in *Malvacipolloides* until the apertural type and number is confirmed.

Etymology. After spines arranged in groups of two.

Genus *Perisyncolporites* Germeraad et al. 1968

Type species *Perisyncolporites pokornyi* Germeraad et al. 1968

***Perisyncolporites verrucosus* sp. nov.**

Fig. 9.1, 9.2

Holotype. Sample 23824, EF V18-1/2, Fig. 9.1 and 9.2.

Diagnosis. Monad; shape spherical; apolar; symmetry radial; syncolporate; colpoids long, connecting pores, marginate, colpi surface ornamented by small verrucae; tectate; stratification unclear, nexine thick, 2 µm, tectum 1–2 µm; verrucate; verrucae short, 1–2 µm tall, of irregular shape, 2–6 µm long, 2–4 µm wide; smaller rounded verrucae interspersed, 2 × 2 µm.

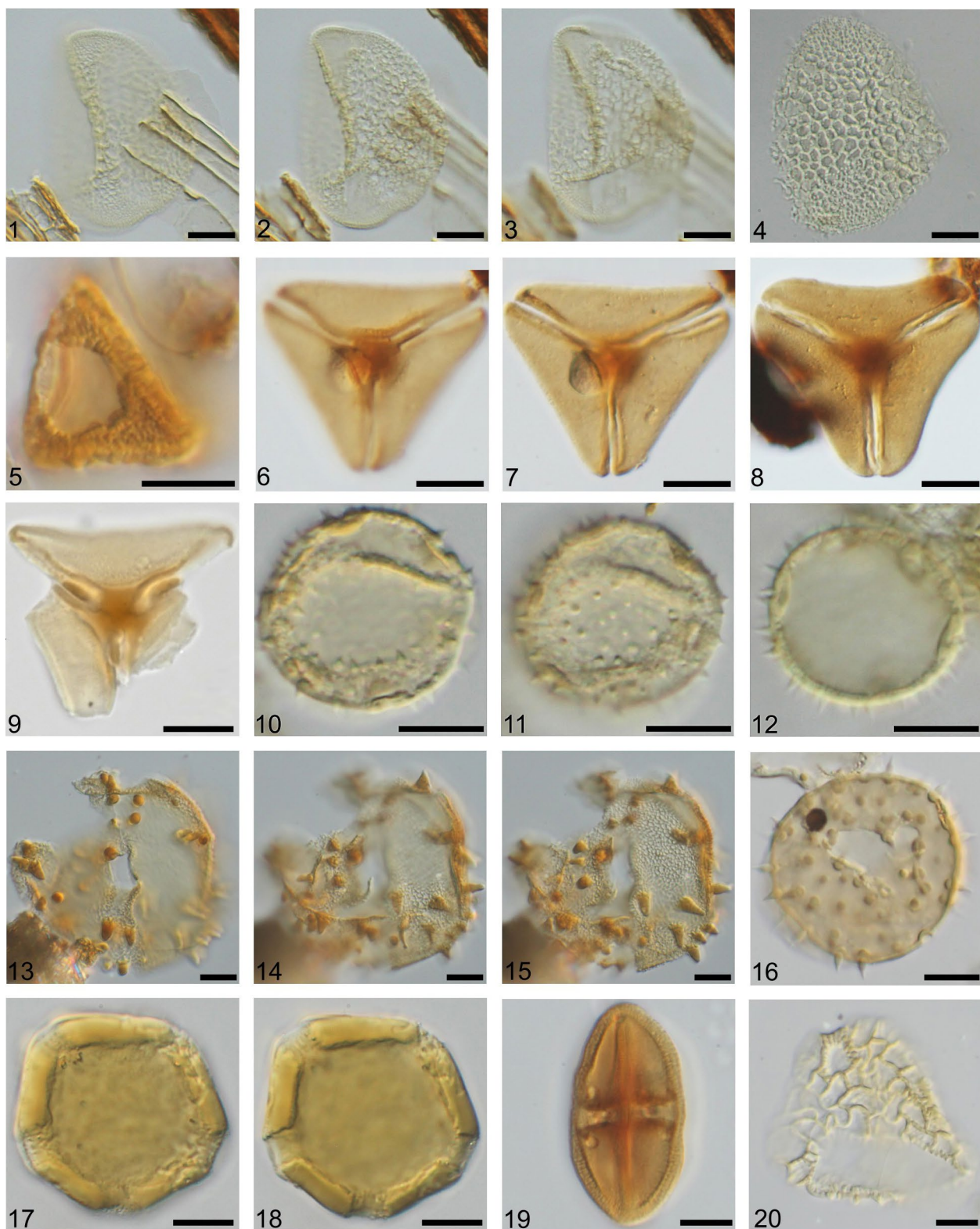


Figure 8. Photomicrographs of pollen from core 1-AS-20-AM, Solimões Basin, western Brazilian Amazonia. **1–3.** *Liliacidites abruptus* sp. nov., holotype, sample 23728, EF J9-1/3; **4.** *Encholirium lymanianum* E. Pereira et Martinelli, Bromeliaceae (CGMS17067_PALMA1315); **5.** *Loranthacites apicirculumreticulatus* Gomes et al. 2021, sample 23956, N11-4; **6–9.** *Loranthacites magnopolaris* sp. nov., **6, 7.** holotype, sample Urumaco-Socorro 1097m, EF H25-2, **8.** paratype, sample Urumaco-Socorro 1440 m, EF O49-1/3, **9.** specimen, sample 23912, EF H12; **10, 11.** *Malvacipollis spinulosa* Frederiksen 1983, sample 23883, EF W7-1; **12.** *Piranhea trifoliata* Baill., Picrodendraceae (CGMS41376_PALMA1214); note the similarity of these two zonoporate grains, *P. trifoliata* is a likely affinity of the fossil *M. spinulosa*; **13–15.** *Malvacipolloides? dupliechinatus* sp. nov., holotype, sample 23811, EF M8-3; **16.** *Mauritiidites franciscoi* var. *franciscoi* (Van der Hammen 1956) Van Hoeken-Klinkenberg 1964, sample 23941, EF U41-1; **17, 18.** *Pachydermites diederixi* Germeraad et al. 1968, sample 23900, EF W19-2/4; **19.** *Paleosantalaceaeapites cingulatus* Jaramillo et al. 2011, sample 23797, EF M39-2; **20.** *Passifloriidites pseudoperculatus* D'Apolito et al. 2021, sample 23811, EF R7. All scale bars = 10 µm

Dimensions. Equatorial view length 32 μm (32–32 μm , $n=1$); equatorial view width 32 μm (32–32 μm , $n=1$); colpi length 16 μm (16–16 μm , $n=1$); colpi width 3 μm (3–3 μm , $n=1$); pore length 4 μm (4–4 μm , $n=1$); pore width 4 μm (4–4 μm , $n=1$).

Comparisons. *Perisyncolporites pokornyi* Germenaad et al. 1968 was described as psilate. However, some very well-preserved specimens have been seen with irregular verrucae, which could reveal morphological variability attributable to known extant species within the Malpighiaceae (see below).

Natural Affinity. *Heteropterys/Mascagnia* (Malpighiaceae) (Fig. 9.3 and 9.4). The periporate spherical morphology with colpoids connecting pores is typical of some Malpighiaceae. Such morphology combined with varying degrees of rugulate/verrucate ornamentation has been described for some genera like *Heteropterys/Mascagnia* (e.g. Gonçalves-Esteves et al., 2007; Belonsi and Gasparino, 2015).

Etymology. After verrucate ornamentation.

Genus *Psilabrevitricolporites*
Van der Kaars 1983

Type species *Psilabrevitricolporites simpliformis* Van der Kaars 1983

Psilabrevitricolporites triangularis
(Van der Hammen et Wymstra 1964)
Jaramillo et Dilcher 2001

Fig. 9.5

Specimen. Sample 23964, EF L38, Fig. 9.5.

Synonyms.

- 1964 *Psilatricolporites triangularis* Van der Hammen and Wymstra, 1964, p. 237, pl. 3, figs 7, 8.
- 1970 *Psilatricolporites molinae* Schuler and Doubinger, 1970
- 1978 *Brevicolporites molinae* (Schuler and Doubinger, 1970) Salard-Cheboldaeff, 1978

Description. Monad; polar shape triangular-obtuse-convex; isopolar; symmetry radial; tricolporate; lalongate; colpi short, borders straight, ends rounded.; tectate; nexine thickens to 2 μm around pores, columellae indistinct; psilate.

Dimensions. Polar view length 25 μm (25–25 μm , $n=2$); colpi length 7 μm (7–7 μm , $n=1$);

pore length 2 μm (2–2 μm , $n=1$); pore width 3 μm (3–3 μm , $n=1$).

Remarks. *Brevicolporites molinae* (Schuler et Doubinger 1970) Salard-Cheboldaeff 1978 is a junior synonym of *Psilabrevitricolporites triangularis*.

Natural Affinity. Apocynaceae/Sapindaceae

Genus *Rhoipites* Wodehouse 1933

Type species *Rhoipites bradleyi*
Wodehouse 1933

***Rhoipites gracilis* sp. nov.**

Fig. 9.11–9.13

Holotype. Sample 23883, EF N29-1, Fig. 9.11–9.13.

Diagnosis. Monad; equatorial shape perprolate; isopolar; symmetry radial; tricolporate; circular; colpi long, 37 μm long, thin, highly invaginated, ends rounded; pores circular, simple; exine semitectate, nexine 1 μm , columellae 1 μm , tectum 1 μm ; columellae slightly shorter at polar area; reticulate; homobrochate; reticulate, lumina 1–1.5 μm , rounded to slightly elongate, muri 1 μm wide, simplicolumellate.

Dimensions. equatorial view length 48 μm (48–48, $n=1$); equatorial view width 20 μm (20–20 μm , $n=1$); colpi length 37 μm (37–37 μm , $n=1$); colpi width 1 μm (1–1 μm , $n=1$); pore length 2 μm (2–2 μm , $n=1$); pore width 2 μm (2–2 μm , $n=1$).

Comparisons. *Crassitricolporites brasiliensis* Herngreen 1972 has thicker nexine; *Paleosantalaceaepites distinctus* Jaramillo et Dilcher 2001 is endocingulate; *Polotricolporites versabilis* Gonzalez 1967 is thinner and has thicker exine at apocolpium; *Foveotricolpites simplex* (Gonzalez 1967) D'Apolito et al. 2021 has a finer reticulate and is tricolporate; *Retritricolporites alexii* Herngreen 1975 is larger and reticulum is supratectate; *R. belmontensis* Regali et al. 1974 has thicker exine at poles and is more coarsely reticulate; *R. ellipticus* van Hoeken-Klinkenberg 1966 is smaller but has larger lalongate pore relative to grain size; *R. exinamplius* Sarmiento 1992 is finely perforated and has thicker exine; *R. mariannae* Gonzalez 1967 is thicker and more coarsely

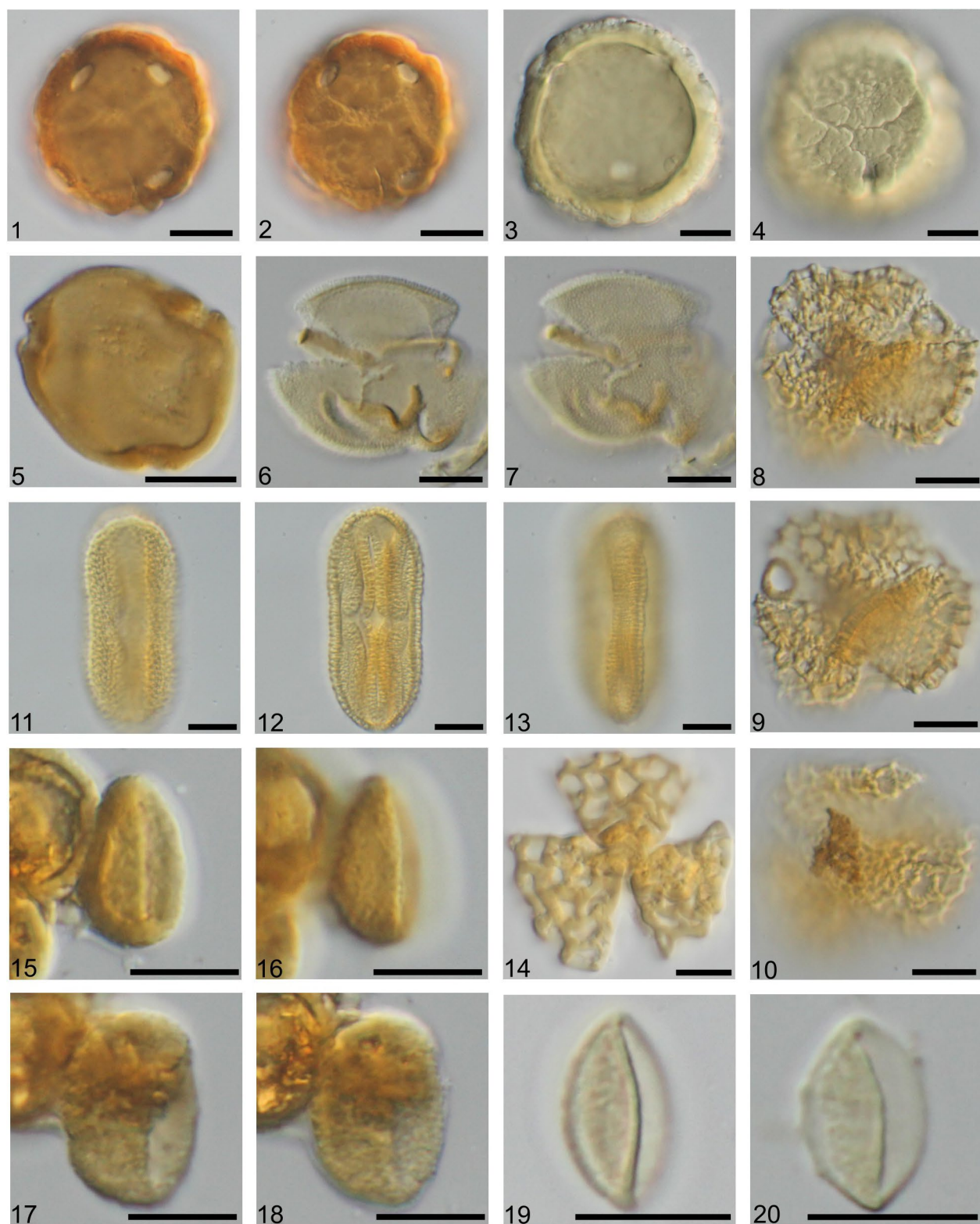


Figure 9. Photomicrographs of pollen from core 1-AS-20-AM, Solimões Basin, western Brazilian Amazonia. **1, 2.** *Perisyncolporites verrucosus* sp. nov., sample 23824, EF V18-1/2; **3, 4.** *Heteropterys afrodisiaca* Machado, Malpighiaceae, UFMT41702_PALMA848; **5.** *Psilabrevitricolporites triangularis* (Van der Hammen et Wymstra 1964) Jaramillo et Dilcher 2001, specimen, sample 23964, EF L38; **6, 7.** *Ranunculacidites pontoreticulatus* D'Apolito et al. 2021, sample 23956, EF W7-3/4; **8–10.** *Rhoipites alfredii* Leite et al. 2021, sample 23811, EF K15-1; **11–13.** *Rhoipites gracilis* sp. nov., holotype, sample 23883, EF N29-1; **14.** *Rousea cavitata* Leite et al. 2021, sample 23856, EF C20; **15, 16.** *Scabramonocolpites bonus* Dueñas 1983, specimen, sample 23840, EF E4-4; **17, 18.** *Scabramonocolpites bonus* Dueñas 1983, specimen, sample 23840, EF E4-4; **19, 20.** *Piper fuligineum* Kunth, Piperaceae (CGMS66120_PALMA1613). All scale bars = 10 µm

reticulate; *R. perpusillus* Regali et al. 1974 is strongly heterobrochate; *Rhoipites guianensis* (Van der Hammen et Wymstra 1964) Jaramillo et Dilcher 2001 is bireticulate, lumina elongate along polar axis; *R. hispidus* (Van der Hammen et Wymstra 1964) Jaramillo et Dilcher 2001 has endexine thinning towards poles and finer reticulate; *Tetracolporopollenites magniporatus* (Hoorn 1993) D'Apolito et al. 2021 is psilate to microreticulate and has large pores; *R. caputoi* (Hoorn 1993) D'Apolito et al. 2021 is microreticulate and has thicker exine relative to grain size; *R. planipolaris* Jaramillo et al. 2010 is smaller and strongly heterobrochate; *Retitricolporites ogowensis* Boltenhagen 1976 has longolongate pores and is strongly heterobrochate; *Cistacearumpollenites rotundiporus* Silva-Caminha et al. 2010 is smaller and finely reticulate; *Retitrescolpites? traversei* Silva-Caminha et al. 2010 has a coarser reticula; *Rhoipites gigantiporus* Silva-Caminha et al. 2010 has much larger pores; *R. negroensis* D'Apolito et al. 2019 has a coarser reticula; *Retitricolporites crucipori* Muller 1968 is heterobrochate; *R. semistriatus* Muller 1968 is striate; *Multiareolites? reticulatus* Leite et al. 2021 has areola.

Etymology. After the slender (gracile) shape.

Genus *Scabramonocolpites* Mathur 1966

Type species *Scabramonocolpites longicolpatus* Mathur 1966

***Scabramonocolpites bonus* Dueñas 1983**

Fig. 9.15–9.18

Specimens. Sample 23840, EF E4-4, Fig. 9.15 and 9.16; sample 23840, EF E4-4, Fig. 9.17 and 9.18.

Description. Monad; polar shape ellipsoidal; isopolar; symmetry bilateral; monosulcate (monocolpate); colpus long, almost as long as polar axis, simple; intectate; exine thickness <1 µm; both positive and negative elements observed; scabrate to micropitted, small scabrae/microverrucate, rounded, ~0.5 µm, pits less common, rounded, ~0.5 µm, elements densely distributed.

Dimensions. Polar view length 21.6 µm (17–30 µm, n=5); polar view width 13 µm (10–16 µm, n=3); colpus length 14.5 µm (14–15 µm, n=2).

Comparisons. *S. abajiensis* Jan du Chene et al. 1978 is larger, thicker, colpus reaches poles and exine is scabrate; *Gemmamonocolpites pilulus* Askin 1994 is larger and gemmae/verrucae larger relative to grain size; *Cycadopites stonei* Helby 1987 is strongly verrucate and colpi ends are open; *Monosulcites chaloneri* Brenner 1963 is strongly verrucate.

Natural Affinity. Piperaceae? (Fig. 9.19 and 9.20). The small-sized and boat-shaped ellipsoid morphology suggests affinity with the Piperaceae. However, extant *Piper* pollen grains, for instance, are even smaller, ranging around 10 µm or less (Fontes et al., 2020; Jaramillo and Rueda, 2023).

Genus *Striamonocolpites* Mathur et Mathur 1969

Type species *Striamonocolpites longicolpatus*
Mathur et Mathur 1969

***Striamonocolpites paludosus* sp. nov.**

Fig. 10.1–10.8

Holotype. Sample 23941, EF S15-3/4, Fig. 10.1–10.3.

Paratype. Sample 23941, EF V39, Fig. 10.4 and 10.5.

Specimen. Sample 23941, EF S40-3, Fig. 10.6–10.8.

Diagnosis. Monad; polar shape ellipsoidal; isopolar; symmetry bilateral; monosulcate (monocolpate); colpus long, reaching poles, often open at ends, marginate, margo created by thinning of exine, both polar and central area often break; exine tectate, nexine ~0.7 µm, columellae ~0.7 µm, thin, regularly spaced, tectum ~0.7 µm thick. Exine thinning towards poles; striate and reticulate; striae thin, ~0.5 µm, nexine surface pitted, pits rounded, very small ~0.5 µm, denser in the central area, gradually becoming heterobrochate smooth toward poles.

Dimensions. Polar view length 53.6 µm (42–58 µm, n=8); polar view width 25.4 µm (22–31 µm, n=8); colpus length 53.6 µm (42–58 µm, n=8).

Comparisons. *Striamonocolpites rectostriatus* Legoux 1978 has much thicker and

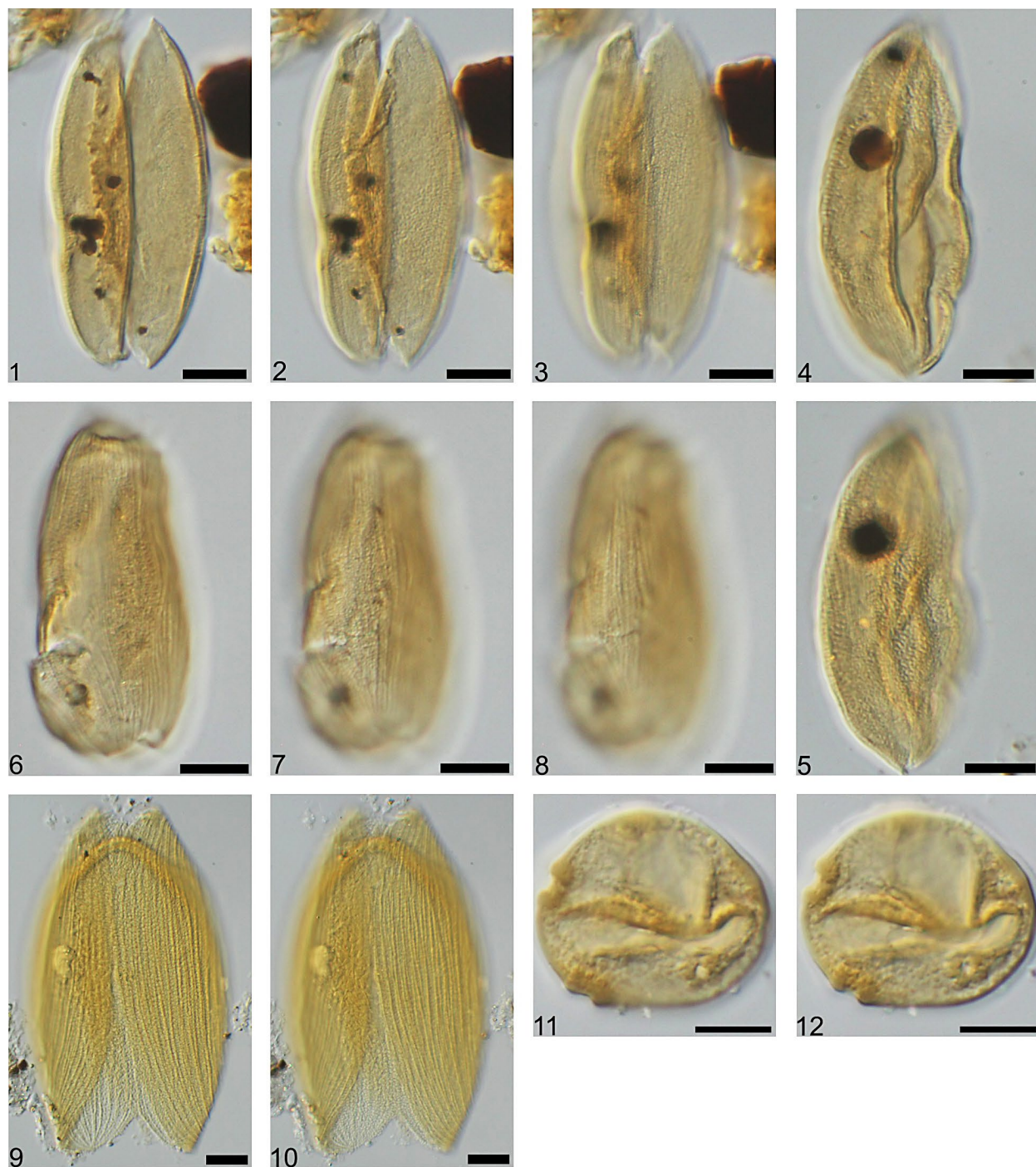


Figure 10. Photomicrographs of pollen from core 1-AS-20-AM, Solimões Basin, western Brazilian Amazonia. **1–3.** *Striamonocolpites paludosus* sp. nov., holotype, sample 23941, EF S15-3/4; **4, 5.** *Striamonocolpites paludosus* sp. nov., paratype, sample 23941, EF V39; **6–8.** *Striamonocolpites paludosus* sp. nov., specimen, sample 23941, EF S40-3; **9, 10.** *Cabomba furcata* Schult. et Schult.f., Cabombaceae (CGMS59302_PALMA1016); **11, 12.** *Verrustephanoporites intraverrucosus* D'Apolito et al. 2021, sample 23941, EF D13-1. All scale bars = 10 µm

well-spaced striae; *S. anastomosus* Boudour-esque 1980 has striae bifurcating and anastomosing; *S. undatostriatus* Legoux 1978 has undulating striae.

Natural Affinity. *Cabomba* (Cabombaceae) (Fig. 10.9 and 10.10). The large monosulcate and striate morphology strongly suggests an affinity with *Cabomba* (Taylor et al., 2008;

Lorente et al., 2017). Monoaperturate-striate grains from other families are different (e.g. Kosenko, 1999; Alzer et al., 2021).

Etymology. after the extant ecology of *Cabomba*, aquatics living in lakes, marshes, and other shallow and slow running waters (Schooler et al., 2009).

DISCUSSION

The biostratigraphic events reported for core 20AM are broadly in agreement with other cores from the Solimões Formation (Fig. 1B), strengthening the idea that such events are comparable basinwide and can be correlated with zonation schemes elsewhere (Germeraad et al., 1968; Lorente 1986; Jaramillo et al., 2011). One novel finding is the occurrence of *C. annulatus* (Fig. 4.7–4.8), proving the existence of the T17 zone in 20AM. This confirms a longer Late Miocene sequence for the Solimões Formation in comparison to previous studies, which could go up to ~7 Ma (Jaramillo et al., 2011).

The occurrence of *F. spinosus* (Fig. 7.8–7.11) is also noteworthy, given this taxon is rare in Amazonia but a zone marker in Colombia and Venezuela (Lorente, 1986; Jaramillo et al., 2011). Its FAD has been observed close to the FAD of *G. magnaclavata* in core 33AM (Leite et al., 2021), which suggests T16 could be thicker than observed (Espinosa et al., 2021) or that some events are older than thought. This will need further testing and appropriate age calibrations. The range of *Ladakhipollenites? caribbiensis* (Fig. 7.17) is evidently long and older than T16, which invalidates this taxon as a marker of the latest Miocene or Pliocene (Leite et al., 2021).

The age assignment of the Içá Formation as T18 in core 20AM is only tentative due to its thin stratigraphy, a single sample and limited amount of palynomorphs found. This zone ranges from 4.8 Ma to modern times, however, is largely affected by an accumulation of LADs attributed to the edge effect (Jaramillo et al., 2011). Given the assumed hiatus between deposition of the Solimões and Içá units, and between Içá and the Holocene cover, we do not base any interpretations on LADs found in the topmost Solimões samples in core 20AM. It is worth noting that the markers *G. magnaclavata* and *C. vanraadshooveni* are absent in the Içá Formation sample, their LADs are estimated at 3.4 Ma (Jaramillo et al., 2011). In addition, *P. cingulatus* has a similar estimated LAD at ~3.7 Ma and was observed. These events are interpreted with caution but could indicate at least a 3 to 4 million years gap between both formations in core 20AM. Absolute OSL dates for the upper part of the Içá Formation are 110,000 years in outcrops in

the region of core 20AM (Pupim et al., 2019) and up to ~220,000 years elsewhere in the basin (Rossetti et al., 2015), which would create and even longer hiatus of ~6 million years. At this stage, it is difficult to reconcile palynology and absolute ages of the topmost Solimões and Içá formations, as the lack of a thick Pliocene sequence impedes that attempt.

One outstanding result from core 20AM is the >61 m of samples with high counts of marine indicators. This contrasts with much thinner marine layers in other cores like 4.7 m in 105AM (Jaramillo et al., 2017) and ~14 m in 9AM (Espinosa et al., 2021). Exceptions are cores 51AM (Leandro et al., 2022) and 46AM (Sá et al., 2020) that have marine indicators intermittently along intervals encompassing >65 m each. These results indicate that the northern part of the Solimões Basin may have been more intensely affected by marine settings in the Middle Miocene than previously thought. Finally, we highlight the importance of the present data for biodiversity analyses – the chronology proposed for core 20AM allows a more complete sequence of the Miocene in western Amazonia. This will let us correlate cores more precisely and have a longer and continuous set of samples to attempt answering important questions like the response of vegetation to landscape and climatic events during the Neogene (e.g. D'Apolito et al., 2021; Hoorn et al., 2022a, b).

ACKNOWLEDGEMENTS

The authors are thankful to CPRM (Brazilian Geological Service) for permit to work on core 20AM and collect samples. We are thankful to Mauricio León for imaging one specimen, and to Manuel Paez Reyes and Dáman Cárdenas for help with dinocyst identifications. We are also thankful to Carina Hoorn and one anonymous reviewer for their helpful comments. CD thanks CNPq (Conselho Nacional de Desenvolvimento Científico e Tecnológico) for postdoctoral grant [150247/2020-6] and FAGEO/UFMT for infrastructure. Thanks to Dr. David Cofrin, the Anders Foundation, Fund 1923, and Gregory D. and Jennifer Walston Johnson.

ADDITIONAL INFORMATION

CONFLICT OF INTEREST. The authors have declared that no competing interests exist.

ETHICAL STATEMENT. No ethical statement was reported.

FUNDING. This research was supported by postdoctoral grant no 150247/2020-6 (to CD).

REFERENCES

- Alzer, F.C., Couto, R.S., Lopes, R.C., Gonçalves-Esteves, V., Mendonça, C.B.F., 2021. Palynotaxonomy of Neotropical species of *Dioscorea* L. (Dioscoreaceae). *Palynology* 45(1), 73–86. <https://doi.org/10.1080/01916122.2019.1690067>
- Antoine, P.-O., Abello, M.A., Adnet, S., Sierra, A.J.A., Baby, P., Billet, G., Boivin, M., Calderón, Y., Candela, A., Chabain, J., Corfui, F., Croft, D.A., Ganerød, M., Jaramillo, C., Klaus, S., Marivaux, L., Navarrete, R.E., Orliac, M.J., Parra, F., Pérez, M.E., Pujos, F., Rage, J.-C., Ravel, A., Robinet, C., Roddaz, M., Tejada-Lara, J.V., Vélez-Juarbe, J., Wesselingh, F.P., Salas-Gismondi, R., 2016. A 60-Million-Year Cenozoic History of Western Amazonian Ecosystems in Contamana, Eastern Peru. *Gondwana Research* 31, 30–59. <https://doi.org/10.1016/j.gr.2015.11.001>
- Anzótegui, L.M., Garalla, S., 1986. Estudio palinológico de la Formación Paraná (Mioceno superior) – “Pozo Josefina” – Provincia de Santa Fe, Argentina. I parte. Descripciones sistemáticas. *FACENA* 6, 101–178.
- Archangelsky, S., 1973. Palinología del Paleoceno de Chubut. I. Descripciones Sistemáticas. *Ameghiniana* 10(4), 339–399.
- Archangelsky, S., Zamalloa, M.C., 1986. Nuevas descripciones palinológicas de las formaciones Salamanca y Bororo, Paleoceno de Chubut (República Argentina). *Ameghiniana* 23(1–2), 35–46.
- Askin, R.A., 1994. Monosulcate angiosperm pollen from the López de Bertodano Formation (upper Campanian–Maastrichtian–Danian) of Seymour Island, Antarctica. *Review of Palaeobotany and Palynology* 81, 151–164. [https://doi.org/10.1016/0034-6667\(94\)90105-8](https://doi.org/10.1016/0034-6667(94)90105-8)
- Belonsi, T.K., Gasparino, E.C., 2015. Pollen morphology of Malpighiaceae from Brazilian forest fragments. *Brazilian Journal of Botany* 38, 379–393. <https://doi.org/10.1007/s40415-015-0134-1>
- Bissaro-Júnior, M.C., Kerber, L., Crowley, J.L., Ribeiro, A.M., Ghilardi, R.P., Guilherme, E., Negri, F.N., Souza-Filho, J.P., Hsiou, A.S., 2019. Detrital zircon U-Pb geochronology constrains the age of Brazilian Neogene deposits from Western Amazonia. *Palaeogeography, Palaeoclimatology, Palaeoecology* 516, 64–70. <https://doi.org/10.1016/j.palaeo.2018.11.032>
- Boltenhagen, E., 1976. Pollen et spores Sénoniens du Gabon. *Cahier de Micropaléontologie* 3, 3–21.
- Boonstra, M., Ramos, M.I.F., Lammertsma, E.I., Antoine, P.O., Hoorn, C., 2015. Marine connections of Amazonia: Evidence from foraminifera and dinoflagellate cysts (early to middle Miocene, Colombia/Peru). *Palaeogeography, Palaeoclimatology, Palaeoecology* 417, 176–194. <https://doi.org/10.1016/j.palaeo.2014.10.032>
- Boudouresque, L., 1980. Contribution de la paléopalynologie à la reconstitution floristique, stratigraphique et paléogéographique de la bordure occidentale du Bassin des Iullemede, au Crétacé supérieur et au Paléogène (Niger et Mali-Afrique de l'Ouest). Thèse 3é Cycle Niamey. Géologie Sédimentaire, 244p.
- Brenner, G.J., 1963. The Spores and Pollen of the Potomac Group of Maryland. Maryland Department of Geology, Mines and Water Resources Bulletin, 27, Baltimore, USA.
- Cárdenas, D., Oboh-Ikuenobe, F., Jaramillo, C., 2021. New acritarch and peridinioid dinoflagellate cyst species from the Oligocene–Miocene of Colombia. *Review of Palaeobotany and Palynology* 290, 104427. <https://doi.org/10.1016/j.revpalbo.2021.104427>
- Cookson, I.C., 1947. Plant microfossils from the lignites of Kerguelen Archipelago. *B.A.N.Z. Antarctic Research Expedition (1929–31) Reports Ser. A2*, 127–142.
- Couper, R.A., 1953. Upper Mesozoic and Cainozoic Spores and Pollen Grains from New Zealand. *New Zealand Geological Survey Palaeontological Bulletin*, 22.
- Cruz, N.M.C., 1984. Palinologia do Linhito do Solimões no Estado do Amazonas. Abstracts of the II Simpósio de Geologia da Amazônia, Manaus, Brazil, 473–480.
- D'Apolito, C., 2024. Raw palynological counts for core 1-AS-20-AM, Miocene–Quaternary of western Amazonia. figshare. Dataset. <https://doi.org/10.6084/m9.figshare.26273662>
- D'Apolito, C., Silva-Caminha, S.A.F., Jaramillo, C., Dino, R., Soares, E.A.A., 2019. The Pliocene–Pleistocene palynology of the Negro River, Brazil, Palynology. *Palynology* 43(2), 223–243.
- D'Apolito, C., Jaramillo, C., Harrington, G., 2021. Miocene palynology of the Solimões Formation (well 1-AS-105-AM), western Brazilian Amazonia. *Smithsonian Contributions to Paleobiology* 105, 1–134. <https://doi.org/10.25573/data.13184924.v2>
- D'Apolito, C., Gomes, B.T., Leite, F.P.R., Silva-Caminha, S.A.F., 2022. Fossil *Parkia* R.Br. (Fabaceae) pollen from the Miocene of western Amazonia. *Grana* 61(6), 401–420. <https://doi.org/10.1080/00173134.2022.2130009>
- de Verteuil, L., Norris, G., 1996. Miocene Dinoflagellate Stratigraphy and Systematics of Maryland and Virginia. *Micropaleontology* 42, 1–172.
- Duenas, H., 1983. Fluctuaciones del nivel del mar durante el depósito de los sedimentos basales de la formación Ciénaga de Oro. *Revista de la Academia Colombiana de Ciencias Exactas, Físicas y Naturales* 15(58), 67–76.
- Eisawi, A., Schrank, E., 2008. Upper Cretaceous to Neogene palynology of the Melut Basin, southeast Sudan. *Palynology* 32, 101–129. <https://doi.org/10.1080/01916122.2008.9989653>
- Elsik, W.C., 1968. Palynology of a Paleocene Rockdale Lignite, Milam County, Texas. II. Morphology and Taxonomy. *Pollen et Spores* 10, 559–664.
- Espinosa, B.S., D'Apolito, C., Silva-Caminha, S.A.F., Ferreira, M.G., Absy, M.L., 2020. Neogene paleoecology and biogeography of a Malvoid pollen in northwestern South America. *Review of Palaeobotany and Palynology* 273, 104131. <https://doi.org/10.1016/j.revpalbo.2019.104131>

- Espinosa, B.S., D'Apolito, C., Silva-Caminha, S.A.F., 2021. Marine influence in western Amazonia during the late Miocene. *Global and Planetary Changes* 205, 103600. <https://doi.org/10.1016/j.gloplacha.2021.103600>
- Feijó, F.J., Souza, R.G., 1994. Bacia do Acre. *Boletim de Geociências da Petrobras* 8, 9–16.
- Fontes, D., Jaramillo, C., Moreno, J.E., 2020. Pollen morphology of the Amacayacu Forest dynamics plot, Western Amazon, Colombia. *Palynology* 44(1), 32–79. <https://doi.org/10.1080/01916122.2018.1538024>
- Germeraad, J.H., Hopping, C.A., Muller, J., 1968. Palynology of Tertiary sediments from tropical areas. *Review of Palaeobotany and Palynology* 6, 189–348. [https://doi.org/10.1016/0034667\(68\)900511](https://doi.org/10.1016/0034667(68)900511)
- Gomes, B.T., Absy, M.L., D'Apolito, C., Jaramillo, C., Almeida, R., 2021. Compositional and diversity comparisons between the palynological records of the Neogene (Solimões Formation) and Holocene sediments of Western Amazonia. *Palynology* 45, 3–14. <https://doi.org/10.1080/01916122.2019.1692314>
- Gomes, B.T., Absy, M.L., D'Apolito, C., Caballero-Rodríguez, D., Martínez, C., Jaramillo, C., 2022. Miocene paleoenvironments and paleoclimatic reconstructions based on the palynology of the Solimões Formation of Western Amazonia (Brazil). *Palynology* 46(2), 1–19. <https://doi.org/10.1080/01916122.2021.1980129>
- Gonçalves-Esteves, V., Soares Junior, E.F., Mendonça, C.B.F., 2007. Palinologia de espécies de Malpighiaceae Juss. ocorrentes nas restingas do Estado do Rio de Janeiro. *Hoehnea* 34(4), 519–529. <https://doi.org/10.1590/S2236-89062007000400007>
- González-Guzmán, A.E., 1967. A palynological Study on the Upper Los Cuervos and Mirador Formations (Lower and Middle Eocene; Tibú area, Colombia). Leiden. E. J. Brill.
- Halbritter, H., 2016. *Encholirium subsecundum*. In: PalDat – A palynological database. https://www.palddat.org/pub/Encholirium_subsecundum/300366?jsessionid=C7E096B8F15177B3C9647185AFEBB00C. Accessed 09 July 2024.
- Halbritter, H., 2016. *Pontederia cordata*. In: PalDat – A palynological database. https://www.palddat.org/pub/Pontederia_cordata/300430?jsessionid=75D3DE1ED9DCDC3F42A75A00BFC9A787. Accessed 08 July 2024.
- Halbritter, H., Heigl H., 2021. *Pedicularis elongata*. In: PalDat – A palynological database. https://www.palddat.org/pub/Pedicularis_elongata/305106. Accessed 08 July 2024.
- Helby, R., 1987. *Muderongia* and related dinoflagellates of the latest Jurassic to Early Cretaceous of Australia. In: Jell, P.A., (ed.), *Studies in Australian Mesozoic Palynology*. Association of Australian Palaeontologists, Memoir 4, Sydney, pp. 297–336.
- Herngreen, G.F.W., 1972. Some new pollen grains from the upper Senonian of Brazil. *Pollen et Spores* 14, 97–112.
- Herngreen, G.F.W., 1975. An Upper Senonian Pollen Assemblage of Borehole 3-Pia 10Al State of Alagoas, Brazil. *Pollen et Spores* 17, 93–140.
- Hoorn, C., 1993. Marine incursions and the influence of Andean tectonics on the Miocene depositional history of northwestern Amazonia: results of a palynostratigraphic study. *Palaeogeography, Palaeoclimatology, Palaeoecology* 105, 267–309. [https://doi.org/10.1016/00310182\(93\)90087-Y](https://doi.org/10.1016/00310182(93)90087-Y)
- Hoorn, C., 1994. Fluvial Palaeoenvironments in the Intracratonic Amazonas Basin (Early Miocene–Early Middle Miocene, Colombia). *Palaeogeography, Palaeoclimatology, Palaeoecology* 109, 1–54. [https://doi.org/10.1016/00310182\(94\)90117-1](https://doi.org/10.1016/00310182(94)90117-1)
- Hoorn, C., Wesselingh, F.P., ter Steege, H., Bermudez, M.A., Mora, A., Sevink, J., Sanmartín, I., Sanchez-Meseguer, A., Anderson, C.L., Figueiredo, J.P., Jaramillo, C., Riff, D., Negri, F.R., Hooghiemstra, H., Lundberg, J., Stadler, T., Sarkinen, T., Antonelli, A., 2010. Amazonia through time: Andean uplift, climate change, landscape evolution, and biodiversity. *Science* 330, 927–931. <https://doi.org/10.1126/science.1194585>
- Hoorn, C., Boschman, L.M., Kukla, T., Sciumbata, M., Val, O., 2022a. The Miocene wetland of western Amazonia and its role in Neotropical biogeography. *Botanical Journal of the Linnean Society* 199(1), 25–35. <https://doi.org/10.1093/botlinnean/boab098>
- Hoorn, C., Kukla, T., Bogotá-Angel, G., van Soelen, E., González-Arango, C., Wesselingh, F.P., Vonhof, H., Val, P., Morcote-Rios, G., Roddaz, M., Dantas, E.L., Santos, R.V., Damsté, J.S.S., Kim, J.-H., Morley, R.J., 2022b. Cyclic sediment deposition by orbital forcing in the Miocene wetland of western Amazonia? New insights from a multidisciplinary approach. *Global and Planetary Change* 210, 103717. <https://doi.org/10.1016/j.gloplacha.2021.103717>
- Hoorn, C., Lohmann, L.G., Boschman, L.M., Condamine, F.L., 2023. Neogene History of the Amazonian Flora: A Perspective Based on Geological, Palynological, and Molecular phylogenetic Data. *Annual Review of Earth and Planetary Sciences* 51, 419–46. <https://doi.org/10.1146/annurev.earth-081522-090454>
- Hu, Z., Zhao, C., Zhao, Y., Liu, J., 2021. Pollen morphology of Liliaceae and its systematic significance. *Palynology* 45(3), 531–568. <https://doi.org/10.1080/01916122.2021.1882601>
- Ibrahim, M., Adbel-Kireem, M.R., 1997. Late Cretaceous palynofloras and foraminifera from Ain El-Wadi area, Farafra Oasis, Egypt. *Cretaceous Research* 18, 633–660.
- Jan du Chene, R.E., Adekogbe, O.S., Adediran, S.A., Petters, S.W., 1978. Palynology and foraminifera of the Lokoja Sandstone (Maastrichtian), Bida Basin, Nigeria. *Revista Española de Micropaleontología* 10(3), 379–393.
- Jaramillo, C.A., Dilcher, D.L., 2001. Middle Paleogene palynology of central Colombia, South America: A study of pollen and spores from tropical latitudes. *Palaeontographica Abt. B* 258, 87–213.

- Jaramillo, C.A., Rueda, M., Torres, V., 2011. A palynological zonation for the Cenozoic of the Llanos and Llanos Foothills of Colombia. *Palynology* 35, 46–84. <https://doi.org/10.1080/01916122.2010.515069>
- Jaramillo, C., Moreno, E., Ramírez V., Silva-Caminha, S.A.F., Barrera, A., Sánchez, C., Morón, S., Herrera, F., Escobar, J., Koll, R., Manchester, S.R., Hoyos, N., 2014. Palynological Record of the Last 20 Million Years in Panama. In: Stevens, W.D., Montiel, O.M., Raven, P. (eds), *Paleobotany and Biogeography: A Festschrift for Alan Graham in His 80th Year*. Missouri Botanical Garden Press, St. Louis, pp. 134–251.
- Jaramillo, C., Romero, I., D'Apolito, C., Bayona, G., Duarte, E., Louwye, S., Escobar, J., Luque, J., Carrillo-Briceño, J.D., Zapata, V., Mora, A., Schouten, S., Zavada, M., Harrington, G., Ortiz, J., Wesselingh, F.P., 2017. Miocene flooding events of western Amazonia. *Science Advances* 3(5), e1601693. <https://doi.org/10.1126/sciadv.1601693>
- Jaramillo, C., Rueda, M.J., 2023. A Morphological Electronic Database of Cretaceous Cenozoic and Extant pollen, spores and dinoflagellates from Northern South America, v. 2023. Available from: <http://biogeodb.stri.si.edu/jaramillosdb/web/morphological/>. Accessed May 2024.
- Kachniasz, K.E., Silva-Caminha, S.A.F., 2016. Palinoestratigrafia da Formação Solimões: comparação entre bioestratigrafia tradicional e o método de Associações Unitárias. *Revista Brasileira de Paleontologia* 19(3), 481–490. <https://doi.org/10.4072/rbp.2016.3.12>
- Kar, R.K., Singh, R.S., 1986. Palynology of the Cretaceous sediments of Meghalaya, India. *Palaeontographica Abt. B* 202(1–6), 83–153.
- Kern, A.K., Gross, M., Galeazzi, C.P., Pupim, F.N., Sawakuchi, A.O., Almeida, R.P., Piller, W.E., Kuhlmann, G.G., Basei, M.A.S., 2020. Re-investigating Miocene age control and paleoenvironmental reconstructions in western Amazonia (northwestern Solimões Basin, Brazil). *Palaeogeography, Palaeoclimatology, Palaeoecology* 545, 109652. <https://doi.org/10.1016/j.palaeo.2020.109652>
- Kosenko, V.N., 1999. Contributions to the pollen morphology and taxonomy of the Liliaceae. *Grana* 38(1), 20–30. <https://doi.org/10.1080/001731300750044672>
- Krutzsch, W., 1959. Mikropaläontologische (sporen-paläontologische) Untersuchungen in der Braunkohle des Geiseltales – [Part] I, Die Sporen und die Sporenartigen sowie ehemals im Geiseltal zu Sporites gestellten Formeinheiten der Sporae dispersae der mitteleozänen Braunkohle des mittleren Geiseltales (Tagebau Neumark-West i.w.S.) unter Berücksichtigung und Revision weiterer Sporenformen aus der bisherigen Literatur. *Geologie*, 8(21/22).
- Latrubesse, E.M., Cozzuol, M., da Silva-Caminha, S.A.F., Rigsby, C.A., Absy, M.L., Jaramillo, C., 2010. The late Miocene paleogeography of the Amazon Basin and the evolution of the Amazon River system. *Earth-Sciences Review* 99, 99–124. <https://doi.org/10.1016/j.earscirev.2010.02.005>
- Leandro, L.M., Vieira, C.E.L., Santos, A., Fauth, G., 2019. Palynostratigraphy of two Neogene boreholes from the northwestern portion of the Solimões Basin, Brazil. *Journal of South American Earth Sciences* 89, 211–218. <https://doi.org/10.1016/j.jsames.2018.11.016>
- Leandro, L.M., Linhares, A.P., De Lira Mota, M.A., Fauth, G., Santos, A., Villegas-Martín, J., Vieira, C.E.L., Bruno, M.D.R., Lee, B., Baecker-Fauth, S., Lopes, F.M., Ramos, M.I.F., 2022. Multi proxy evidence of Caribbean-sourced marine incursions in the Neogene of Western Amazonia, Brazil. *Geology* 50, 465–69. <https://doi.org/10.1130/G49544.1>
- Legoux, O., 1978. Quelques espèces de pollen caractéristiques du Néogène du Nigéria. *Bulletin des Centres de Recherche Exploration-Production Elf-Aquitaine* 2, 265–317.
- Leite, F.P.R., Paz, J., do Carmo, D.A., Silva-Caminha, S.A., 2017. The effects of the inception of Amazonian transcontinental drainage during the Neogene on the landscape and vegetation of the Solimões Basin, Brazil. *Palynology* 41, 412–422. <https://doi.org/10.1080/01916122.2016.1236043>
- Leite, F.P.R., da Silva-Caminha, S.A.F., D'Apolito, C., 2021. New Neogene index pollen and spore taxa from the Solimões Basin (western Amazonia), Brazil. *Palynology* 45, 115–141. <https://doi.org/10.1080/01916122.2020.1758971>
- Linhares, A.P., Ramos, M.I., Gaia, V.C., Friaes, Y.S., 2019. Integrated biozonation based on palynology and ostracods from the Neogene of Solimões Basin, Brazil. *Journal of South American Earth Sciences* 91, 57–70. <https://doi.org/10.1016/j.jsames.2019.01.015>
- Lorente, F.L., Buso Junior, A.A., Oliveira, P.E. de, Pessenda, L.C.R., 2017. Atlas palinológico: laboratório 14C – CENA/USP = Palynological atlas: 14C laboratory – CENA/USP. Piracicaba: FEALQ. 333p.
- Lorente, M., 1986. Palynology and Palynofacies of the Upper Tertiary in Venezuela. *Dissertationes Botanicae* 99. Berlin/Stuttgart, Cramer.
- Maia, R.G., Godoy, H.K., Yamaguti, H.S., Moura, P.A., Costa, F.S., Holanda, M.A., Costa, J., 1977. Projeto de carvão no Alto Solimões: Relatório final. Manaus: CPRM-DNPM, 137p.
- Mathur, Y.K., 1966. On the Microflora in the Supratrappeans of Western Kutch, India. *Quarterly Journal of The Geological, Mining and Metallurgical Society of India* 38, 33–51.
- Mathur, Y.K., Mathur, K., 1969. Studies on the fossil flora of Kutch (India) 3. On the paleo-palynoflora in the Pliocene sediments of Naera-Baraia area, Kutch. *Quarterly Journal of The Geological, Mining and Metallurgical Society of India* 42, 1–12.
- Mathur, Y.K., Jain, A.K., 1980. Palynology and Age of the Dras Volcanics near Shergol, Ladakh, Jammu and Kashmir, India. *Geoscience Journal* 1, 55–74.
- McIntyre, D.J., 1968. Further new pollen species from New Zealand Tertiary and uppermost Cretaceous deposits. *New Zealand Journal of Botany* 6, 177–204.

- Muller, J., 1968. Palynology of the Pedawan and Plateau Sandstone Formations (Cretaceous-Eocene) in Sarawak, Malaya. *Micropaleontology* 14, 1–37.
- Muller, J., Giacomo, E., Van Erve, A.W., 1987. A palynological zonation for the Cretaceous, Tertiary and Quaternary of Northern South America. American Association of Stratigraphic Palynologists Contribution Series 19, 7–76.
- Negri, F.R., Bocquentin-Villanueva, J., Ferigolo, J., Antoine, P.-O., 2010. A review of Tertiary mammal faunas and birds from western Amazonia. In: Hoorn, C., Wesselingh, F.P., (eds), *Amazonia: landscapes and species evolution: a look into the past*. Wiley Blackwell, Oxford, pp. 245–258.
- Nichols, D.J., Ames, H.T., Traverse, A., 1973. On *Arecipites* Wodehouse, *Monocolpopollenites* Thomson & Pflug, and the Species "*Monocolpopollenites tranquillus*". *Taxon* 22, 241–56.
- Ortiz, J., Jaramillo, C., 2020. SDAR: a Toolkit for Stratigraphic Data Analysis. R package version 0.9-55.
- Paiva, A.L.S., Godoy, P.L., Souza, R.B.B., Klein, W., Hsiou, A.S., 2022. Body size estimation of Caimaninae specimens from the Miocene of South America. *Journal of South American Earth Sciences* 118, 103970. <https://doi.org/10.1016/j.jsames.2022.103970>
- Penny, J.H.J., 1986. An Early Cretaceous angiosperm pollen assemblage from Egypt. *Special Papers in Palaeontology* 35, 121–134.
- Pflanzl, G., 1956. Das Alter der Braunkohlen des Meißners, der Flöze 2 und 3 des Hirschberger und eines benachbarten Kohlenlagers bei Laudenbach. *Notizblatt des Hessischen Landesamtes für Amt Bodenforsch zu Wiesbaden* 84, 232–244.
- Pierce, R.L., 1961. Lower Upper Cretaceous Plant Microfossils from Minnesota. *Minnesota Geological Survey Bulletin* 42, 1–86.
- Potonié, R., 1958. Synopsis der Gattungen der Sporae dispersae. II. Teil: Sporites (Nachtrage), Saccites, Aletes, Praecolpates, Polyppicates, Monocolpates. Hannover: Beihefte zum Geologischen Jahrbuch 31.
- Potonié, R., 1966. Synopsis der Gattungen der Sporae dispersae. IV. Teil: Nachtrage zu allen Gruppen (Turmae). Hannover: Beihefte zum Geologischen Jahrbuch 72.
- Punt, W., Hoen, P.P., Blackmore, S., Nilsson, S., Le-Thomas, A., 2007. Glossary of Pollen and Spore Terminology. *Review of Paleobotany and Palynology* 143, 1–81. <https://doi.org/10.1016/j.revpalbo.2006.06.008>
- Pupim, F.N., Sawakuchi, A.O., Almeida, R.P., Ribas, C.C., Kern, A.K., Hartmann, G.A., Chiessi, C.M., Tamura, L.N., Mineli, T.D., Savian, J.F., Grohmann, C.H., Bertassoli, D.J., Stern, A.G., Cruz, F.W., Cracraft, J., 2019. Chronology of Terra Firme formation in Amazonian lowlands reveals a dynamic Quaternary landscape. *Quaternary Science Reviews* 210, 154–163. <https://doi.org/10.1016/j.quascirev.2019.03.008>
- Regali, M.P.S., 1989. *Complicatisaccus cearensis*: uma palinofauna do Eocretáceo do Brasil. 11th Congresso Brasileiro de Paleontologia, Curitiba (1), 235–274.
- Regali, M.S., Uesegui, N., Santos, A., 1974. Palinologia dos sedimentos Meso-Cenozoicos do Brasil (I). *Boletim Técnico da Petrobras* 17, 263–362.
- Reis, N.J., Almeida, M.E., Riker, S.L., Ferreira, A.L., 2006. Geologia e recursos minerais do Estado do Amazonas (texto explicativo dos mapas geológicos e de recursos minerais do Estado do Amazonas). Serviço Geológico do Brasil-CPRM, Manaus.
- Riding, J.B., 2021. A guide to preparation protocols in palynology. *Palynology* 45(1), 1–110. <https://doi.org/10.1080/01916122.2021.1878305>
- Rossetti, D.F., Cohen, M.C., Tatumi, S.H., Sawakuchi, A.O., Cremon, É.H., Mittani, J.C., Bertani, T.C., Munita, C.J.A.S., Tudela, D.R.G., Yee, M., Moya, G., 2015. Mid-Late Pleistocene OSL chronology in western Amazonia and implications for the transcontinental Amazon pathway. *Sedimentary Geology* 330, 1–15. <https://doi.org/10.1016/j.sedgeo.2015.10.001>
- Sá, N.P., Carvalho, M.A., Correia, G.C., 2020. Miocene paleoenvironmental changes in the Solimões Basin, western Amazon, Brazil: a reconstruction based on palynofacies analysis. *Palaeogeography, Palaeoclimatology, Palaeoecology* 537, 109450. <https://doi.org/10.1016/j.palaeo.2019.109450>
- Sah, S.C.D., Dutta, SK., 1966. Palynostratigraphy of the Sedimentary Formations of Assam-1. Stratigraphical Position of the Cherra Formation. *Palaeobotanist* 15(1–2), 72–86.
- Salard-Cheboldaeff, M., 1978. Sur la palynoflore maastrichtienne et tertiaire du basin sédimentaire littoral du Cameroun. *Pollen et Spores* 20(2), 215–260.
- Samoilovich, S.R., Mtchedlishvili, N.D., 1961. Pyl'tsa i spory zapadnoi Sibiri:yura-Paleotsen. Leningrad, Russia. Vserossiyskiy Neftyanoy Nauchno-Issledovatel skiy Geologorazvedochnyy Institut 177.
- Santos, V.L., Wanderley, M.G.L., Versieux, L.M., Luz, C.F.P., 2019. Pollen morphology of Brazilian species of *Vriesea* (Bromeliaceae, Tillandsioideae). *Grana* 59(2–3), 203–225. doi.org/10.1080/00173134.2019.1676305
- Sarmiento, G., 1992. Palinología de la Formación Guaduas – Estratigrafía y sistemática. *Boletín Geológico* 32, 45–126.
- Schooler, S., Cabrera-Walsh, W., Julien, M., 2009. *Cabomba caroliniana* Gray (Cabombaceae). In: Muniappan, R., Reddy, G.V.P., Raman, A., (eds), *Biological Control of Tropical Weeds Using Arthropods*. Cambridge University Press, Cambridge, 88–107.
- Schuler, M., Doubinger, J., 1970. Observations palynologiques dans le Basin d'Amaga (Colombie). *Pollen et Spores* 12(3), 429–450.
- Silva-Caminha, S.A.F., Jaramillo, C., Absy, M.L., 2010. Neogene palynology of the Solimões Basin, Brazilian Amazonia. *Palaeontographica Abteilung B* 283, 1–67. <https://doi.org/10.1127/palb/284/2010/13>

- Silva-Caminha, S.A.F., D'Apolito, C., Jaramillo, C., Espinosa, B.S., Rueda, M., 2020. Palynostratigraphy of the Ramon and Solimões Formation in the Acre Basin, Brazil. *Journal of South American Earth Sciences* 103, 102720. <https://doi.org/10.1016/j.jsames.2020.102720>
- Souza S. de O., de Oliveira, R.S., Aona, L.Y.S., Souza, F.V.D., Soares, T.L., Rossi, M.L., Souza, E.H., 2021. Pollen morphology and viability of *Tillandsia* (Bromeliaceae) species by light microscopy and scanning electron microscopy. *Microscopy Research and Technique* 84, 441–459. <https://doi.org/10.1002/jemt.23601>
- Srivastava, S.K., 1977. Microspores from the Fredericksburg Group (Albian) of the southern United States. *Paléobiologie Continentale* 6(1975), 1–119.
- Stover, L.E., Partridge, A.D., 1973. Tertiary and Late Cretaceous spores and pollen from the Gippsland Basin, southeastern Australia. *Royal Society of Victoria* 85(2), 237–286.
- Taylor, M.L., Gutman, B.L., Melrose, N.A., Ingraham, A.M., Schwartz, J.A., Osborn, J.M., 2008. Pollen and anther ontogeny in *Cabomba caroliniana* (Cabombaceae, Nymphaeales). *American Journal of Botany* 95(4), 399–413.
- Ulrich, S., Hesse, M., Bröderbauer, D., Bogner, J., Weber, M., Halbritter, H., 2013. *Calla palustris* (Araceae): New palynological insights with special regard to its controversial systematic position and to closely related genera. *Taxon* 62(4), 701–712. <https://doi.org/10.12705/624.34>
- Van der Hammen, T., 1956. A Palynological Systematic Nomenclature. *Boletín Geológico* 4, 63–101.
- Van der Hammen, T., Wymstra, T.A., 1964. A Palynological Study on the Tertiary and Upper Cretaceous of British Guayana. *Leidse Geologische Mededelingen* 30, 183–241.
- Van der Kaars, W.A., 1983. A Palynological-Paleoecological Study of the Lower Tertiary Coal-Bed Sequence from El Cerrejón (Colombia). *Geología Norandina* 8, 33–48.
- Van Hoek-Klinkenberg, P.M.J., 1964. A Palynological Investigation of Some Upper Cretaceous Sediments in Nigeria. *Pollen et Spores* 6, 209–231.
- Van Hoek-Klinkenberg, P.M.J., 1966. Maastrichtian Paleocene and Eocene Pollen and Spores from Nigeria. *Leidse Geologische Mededelingen* 38, 37–48.
- Venkatachala, B.S., Kar, R.K., 1969. Palynology of the Tertiary sediments of Kutch-I. Spores and pollen from bore hole no.14. *Palaeobotanist* 17, 157–178.
- Wall, D., 1967. Fossil Microplankton in Deep-Sea Cores from the Caribbean Sea. *Palaeontology* 10(1), 95–123.
- Wanderley-Filho, J.R., Eiras, J.F., Vaz, P.T., 2007. Bacia do Solimões. *Boletim de Geociências da Petrobrás* 15, 217–225.
- Wesselingh, F.P., Ramos, M.I., 2010. Amazonian Aquatic Invertebrate Faunas (Mollusca, Ostracoda) and Their Development Over the Past 30 Million Years. In: Hoorn, C., Wesselingh, F.P., (eds), *Amazonia: Landscape and Species Evolution – A Look into the Past*. Blackwell Publishing, Oxford, 302–316.
- Wesselingh, F.P., Anderson, L.C., Kadolsky, D., 2006. Molluscs from the Miocene Pebas Formation of Peruvian and Colombian Amazonia. *Scripta Geologica* 133, 19–290.
- Wodehouse, R.P., 1933. The Oil Shales of the Eocene Green River Formation. *Bulletin of the Torrey Botanical Club* 60, 479–535.
- Zavada, M.S., 1983. Comparative Morphology of Monocot Pollen and Evolutionary Trends of Apertures and Wall Structures. *The Botanical Review* 49(4), 331–379.